

Designing Novel Benzofuran Derived AIE-probe: Dual-Mode Fluorescence Turn-Off and Naked-Eye Color Change for Hydrazine Detection

Gauravi Yashwantro,^a Anjali Tripathi,^b Saona Seth,^c Purav Badani^b and Satyajit Saha*^a

^aDepartment of Speciality Chemicals Technology, Institute of Chemical Technology, Mumbai, Maharashtra-400019, India

^bDepartment of Chemistry, University of Mumbai, Kalina Campus, Mumbai, Maharashtra, India

^cDepartment of Applied Sciences, Tezpur University, Assam, India

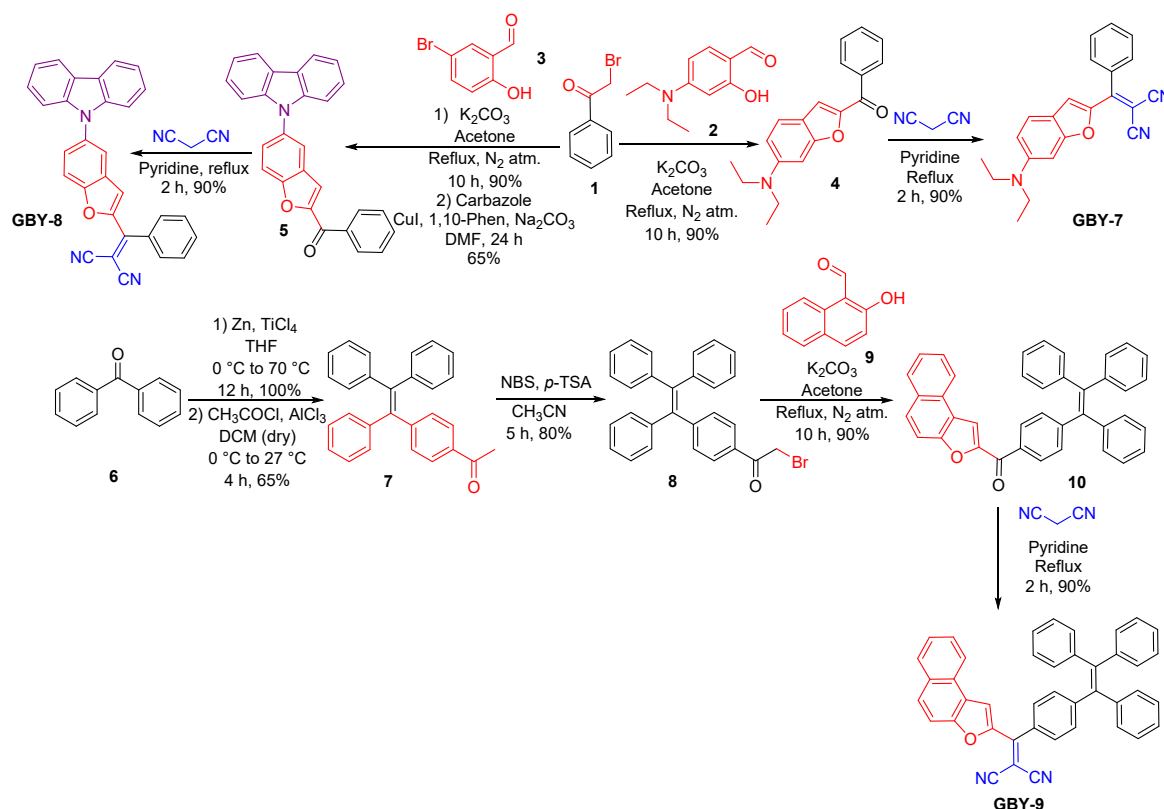
Table of Contents

General aspects.....	S2
Synthetic Scheme and Procedures.....	S2-S5
Characterization data.....	S6
DSC-TGA of GBY-7, GBY-8 and GBY-9	S7
Photophysical Properties of GBY-7, GBY-8 and GBY-9	S7-S8
Solvatochromism of GBY-7, GBY-8 and GBY-9	S8-S9
Aggregation Induced Emission Studies of GBY-7, GBY-8 and GBY-9	S9-S11
DLS analysis GBY-7, GBY-8 and GBY-9	S11-S12
SEM analysis of GBY-7, GBY-8 and GBY-9, Tyndall effect	S12
Fluorescence Quantum yield Calculation of GBY-7, GBY-8 and GBY-9	S12-S14
Cyclic Voltammetry Analysis of GBY-7, GBY-8 and GBY-9	S14-S15
DFT Calculations.....	S16-S25
Hydrazine sensing GBY-7, GBY-8 and GBY-9	S25-S29
References.....	S29-S30
¹ H and ¹³ C NMR Spectral Reproductions Of 8, 10, GBY-7, GBY-8 and GBY-9 ...	S31-S35
LC-HRMS data of 8, 10, GBY-7, GBY-8 and GBY-9	S36-S37
Single Crystal X-Ray Data of GBY-7, GBY-9	S37-S52

General aspects

All chemicals were purchased from available commercial sources like Sigma-Aldrich, Spectrochem, and S. D. Fine chemicals and used without further purification. Organic solvents were dried and distilled before use. Silica gel-coated aluminium sheets (ACME, 254F) were used for the Thin Layer Chromatography (TLC) analysis using ethyl acetate and petroleum ether as the eluents to monitor the reaction progress. Melting points of all the compounds were recorded by the AnalabThermoCal melting point apparatus in the open capillary tube. Fourier transform infrared (FTIR) (ATR-IR) spectra were obtained with Alpha-II/Bruker-instrument. The ^1H Nuclear Magnetic Resonance (^1H NMR) spectroscopy was carried out on Bruker 400 spectrometer whereas ^{13}C NMR was carried out on 100 MHz spectrometer using CDCl_3 as a solvent. Chemical shifts are reported in parts per million (ppm) downfield from TMS, and the spin multiplicities are described as s (singlet), d (doublet), t (triplet), and multiplet (m). Coupling constant (J) values are reported in hertz (Hz). Thermogravimetric analysis (TGA) was conducted on a Perkin-Elmer Diamond TG/DTA instrument at a heating rate of $10^\circ\text{C}/\text{min}$ under a nitrogen atmosphere with a flow rate of $150\text{ mL}/\text{min}$. UV-Visible absorption spectra were obtained on a FP-8200/Jasco spectrophotometer. Cyclic voltammetry (CV) measurements were measured in an electrolyte solution of tetrabutylammonium hexafluorophosphate (Bu_4NPF_6) in DMF (0.1 M), using platinum gauze and Ag/AgCl as the counter and reference electrodes respectively. A scan rate of $25\text{ mV}/\text{s}$ was used during the CV measurements.

General procedure for the Synthesis and the Characterization Data of GBY-7, GBY-8 and GBY-9



Scheme S1. Synthetic route for the preparation of GBY-7, GBY-8 and GBY-9.

Synthesis of (6-(diethylamino)benzofuran-2-yl)(phenyl)methanone (4)^[5] : In a two necked round bottom flask equipped with condenser and magnetic stir bar, 2 4-(diethylamino)salicylaldehyde **2** (0.5 g, 2.58 mmol), and potassium carbonate (1.07 g, 7.74 mmol) were taken in 15 mL of acetone under nitrogen atmosphere. The reaction mixture was stirred for 10 min and then 2-Bromoacetophenone **1** (0.56 g, 2.84 mmol) was added followed by refluxing for 10 h. The progress of the reaction was monitored by TLC analysis. On disappearance of the starting material, excess of the solvent was evaporated under reduced pressure, and water was added to the reaction mass and extracted in ethyl acetate (3*20 ml). The combined organic layer was washed with saturated brine solution and dried over anhydrous sodium sulphate. The organic layer was evaporated under reduced pressure to get hold of the crude product which was subsequently purified by silica gel column chromatography using petroleum ether: ethyl acetate (90:10) as eluent to obtain 0.68 g of **4** in 90% yield.

Synthesis of (5-(9H-carbazol-9-yl)benzofuran-2-yl)(phenyl)methanone (5) : In a two necked round bottom flask equipped with condenser and magnetic stir bar, 5-bromo-2-hydroxybenzaldehyde **3** (0.4 g, 1.98 mmol), and potassium carbonate (1.10 g, 7.9 mmol) were taken in 15 mL of acetone under nitrogen atmosphere. The reaction mixture was stirred for 10 min and then 2-Bromoacetophenone **1** (0.41 g, 2.08 mmol) was added followed by refluxing for 10 h. The progress of the reaction was monitored by TLC analysis. On disappearance of the starting material, excess of the solvent was evaporated under reduced pressure, and water was added to the reaction mass and extracted in ethyl acetate (3*20 ml). The combined organic layer was washed with saturated brine solution and dried over anhydrous sodium sulphate. The organic layer was evaporated under reduced pressure to get hold of the crude product which was subsequently purified by silica gel column chromatography using petroleum ether: ethyl acetate (92:8) as eluent to obtain 0.53 g of intermediate in 90% yield.

In a sealed tube equipped with magnetic stir bar, 10 mL dry DMF was added and purge with N₂ gas for 30 min. Then, (5-bromobenzofuran-2-yl)(phenyl)methanone (0.3 g, 0.99 mmol), potassium carbonate (0.41 g, 2.98 mmol), carbazole (0.17 g, 1.03 mmol), CuI (0.09 g, 0.49 mmol), 1,10-phenanthroline (0.08 g, 0.49 mmol) were added in presence of nitrogen atm. The reaction mixture was stirred for 36 h at 120 °C. After completion of reaction was added to the reaction mass and extracted in ethyl acetate (3*20 ml). The combined organic layer was washed with saturated brine solution and dried over anhydrous sodium sulphate. The organic layer was evaporated under reduced pressure to get hold of the crude product which was subsequently purified by silica gel column chromatography using petroleum ether: ethyl acetate (80:20) as eluent to obtain 0.25 g of **5** in 65% yield.

Synthesis of 2-(((6-(diethylamino)benzofuran-2-yl)(phenyl)methylene)malononitrile (GBY-7): In a round bottom flask equipped with condenser and magnetic stir bar, pyridine 1.5 ml and malononitrile (0.099 g, 1.5 mmol) were stirred for 10 min and then (6-(diethylamino)benzofuran-2-yl)(phenyl)methanone **4** (0.2 g, 0.68 mmol), was added and refluxed for 3 h. After completion of the reaction as observed from the TLC analysis, water was added to the reaction mixture and extracted in ethyl acetate (4*20 ml). The combined organic layer was washed with saturated brine solution and dried over anhydrous sodium

sulphate. The organic layer was evaporated under reduced pressure to get hold of the crude product which was further purified by silica gel column chromatography using petroleum ether: ethyl acetate (82:18) as eluent to obtain 0.20 g of **GBY-7** in 90% yield.

Synthesis of 2-((5-(9H-carbazol-9-yl)benzofuran-2-yl)(phenyl)methylene)malononitrile (GBY-8): In a round bottom flask equipped with condenser and magnetic stir bar, pyridine 1.5 ml and malononitrile (0.074 g, 1.13 mmol) were stirred for 10 min and then (5-(9H-carbazol-9-yl)benzofuran-2-yl)(phenyl)methanone **5** (0.2 g, 0.51 mmol), was added and refluxed for 3 h. After completion of the reaction as observed from the TLC analysis, water was added to the reaction mixture and extracted in ethyl acetate (4*20 ml). The combined organic layer was washed with saturated brine solution and dried over anhydrous sodium sulphate. The organic layer was evaporated under reduced pressure to get hold of the crude product which was further purified by silica gel column chromatography using petroleum ether: ethyl acetate (80:20) as eluent to obtain 0.20 g of **GBY-8** in 90% yield.

Synthesis of 2-bromo-1-(4-(1,2,2-triphenylvinyl)phenyl)ethan-1-one (8): In a two necked round bottom flask fitted with a magnetic stir bar, 80 ml of dry THF was taken under inert atmosphere followed by the addition of zinc powder (7.53 g, 115.3 mmol). The reaction mixture was purged with nitrogen and stirred for 10 mins. The reaction mixture was cooled to -5 °C and dropwise TiCl₄ (7.2 ml, 65.8 mmol) was added. On completion of the addition, the reaction mixture was additionally stirred at room temperature for 30 mins and then refluxed for 2.5 h. The reaction mixture was then cooled to 0 °C and benzophenone **6** (6.0 g, 32.9 mmol) in THF was added dropwise followed by refluxing for 12 h. The progress of the reaction was monitored by TLC and on disappearance of the starting material, the reaction mixture was quenched with 70 ml of 10% potassium carbonate solution and extracted with ethyl acetate (5*50 ml). The organic layer was collected, washed with saturated brine solution, and then dried over anhydrous sodium sulphate and filtered. The organic layer was evaporated under reduced pressure to obtain the desired product tetraphenylethene in 100% yield (10.9 g). Melting point: 220-222 °C. ^[1] The product was flushed through silica gel column and used directly for the next reaction to synthesize 2-1-(4-(1,2,2-triphenylvinyl)phenyl)ethan-1-one (**7**).

Compound **7** was prepared using modified synthetic protocol. 10 ml dry DCM was taken in a three necked round bottom flask equipped with two dropping funnels. In one dropping funnel tetraphenylethene (5.0 g, 15.0 mmol) in 10 ml dry DCM was taken and in the other dropping funnel mixture of acetyl chloride (1.7 ml, 22.5 mmol) and AlCl₃ (3.50 g, 26.3 mmol) in 20 ml dry DCM was taken. The reaction was initiated on simultaneous addition of both the components maintaining the flow rate at 2 ml per minute at 0 °C to 5 °C. Once the addition was over, the reaction mass was stirred at room temperature for 3-4 h and the progress of the reaction was monitored by TLC analysis. On completion of the reaction, the reaction mixture was quenched with 60 mL of cold water and extracted with DCM (5*15 ml). The organic layer was washed with saturated brine solution and dried over anhydrous sodium sulphate. The organic layer was evaporated under reduced pressure to obtain crude 2-1-(4-(1,2,2-triphenylvinyl)phenyl)ethan-1-one (**7**) which was then purified by silica gel column

chromatography using petroleum ether: ethyl acetate (98:2) as eluent to obtain 3.65 g of the (4-(1,2,2-triphenylvinyl)phenyl)ethan-1-one **7** in 65% yield; melting point: 110-112 °C. The characterization data of the product matched with the reported data. [2]

2-bromo-1-(4-(1,2,2-triphenylvinyl)phenyl)ethan-1-one **8** was prepared by bromination of (4-(1,2,2-triphenylvinyl)phenyl)ethan-1-one **7**. In a 2 necked round bottom flask equipped with condenser and magnetic stir bar, **7** (3.5 g, 9.34 mmol), NBS (1.9 g, 11.21 mmol), *p*-TSA (3.5 g, 20.56 mmol) were taken in 30 ml acetonitrile under inert atmosphere. The reaction mixture was then heated to reflux for 4-5 h. The progress of the reaction was monitored by the TLC and on disappearance of the starting material, the reaction mixture was quenched by the addition of cold water and extracted in ethyl acetate (3*25 ml). The combined organic layer was washed with saturated brine solution and dried over anhydrous sodium sulphate. The organic layer was evaporated under reduced pressure to isolate the crude 4.2 g which was then purified by silica gel column chromatography using petroleum ether: ethyl acetate (95:5) as eluent to obtain 3.3 g of 2-bromo-1-(4-(1,2,2-triphenylvinyl)phenyl)ethan-1-one (**8**) in 80% yield.

Synthesis of naphtho[2,1-b]furan-2-yl(4-(1,2,2-triphenylvinyl)phenyl)methanone (10): In a 2 necked round bottom flask equipped with condenser and magnetic stir bar, 2-hydroxy-1-naphthaldehyde **9** (0.25 g, 1.45 mmol), and potassium carbonate (0.5 g, 3.62 mmol) were taken in 15 mL of acetone under nitrogen atmosphere. The reaction mixture was stirred for 10 min and then 2-bromo-1-(4-(1,2,2-triphenylvinyl)phenyl)ethan-1-one **8** (0.68 g, 1.52 mmol) was added followed by refluxing for 10 h. The progress of the reaction was monitored by TLC analysis. On disappearance of the starting material, excess of the solvent was evaporated under reduced pressure, and water was added to the reaction mass and extracted in ethyl acetate (3*20 ml). The combined organic layer was washed with saturated brine solution and dried over anhydrous sodium sulphate. The organic layer was evaporated under reduced pressure to get hold of the crude product which was subsequently purified by silica gel column chromatography using petroleum ether: ethyl acetate (95:5) as eluent to obtain 0.67 g of **10** in 90% yield.

Synthesis of 2-(naphtho[2,1-b]furan-2-yl(4-(1,2,2-triphenylvinyl)phenyl)methylene)malononitrile (GBY-9): In a round bottom flask equipped with condenser and magnetic stir bar, pyridine 1.5 ml and malononitrile (0.063 g, 0.94 mmol) were stirred for 10 min and then naphtho[2,1-b]furan-2-yl(4-(1,2,2-triphenylvinyl)phenyl)methanone **10** (0.2 g, 0.37 mmol), was added and refluxed for 2 h. After completion of the reaction as observed from the TLC analysis, water was added to the reaction mixture and extracted in ethyl acetate (4*20 ml). The combined organic layer was washed with saturated brine solution and dried over anhydrous sodium sulphate. The organic layer was evaporated under reduced pressure to get hold of the crude product which was further purified by silica gel column chromatography using petroleum ether: ethyl acetate (80:20) as eluent to obtain 0.195 g of **GBY-9** in 90% yield.

Characterization Data of 8, 10, GBY-7, GBY-8 and GBY-9

2-Bromo-1-(4-(1,2,2-triphenylvinyl)phenyl)ethan-1-one (8): Yield: 3.3 g, 80%; Melting point: (155-158) °C. IR (AT-IR): 3078, 3022, 2929, 1687, 1550, 1488, 986, 693 cm^{-1} ; ^1H NMR (400 MHz, CDCl_3) δ (in ppm) 4.36 (s, 2H), 6.95 – 7.05 (m, 6H), 7.06 – 7.18 (m, 11H), 7.70 (d, $J = 8.0$ Hz, 2H); ^{13}C NMR (101 MHz, CDCl_3) δ (in ppm) 30.9, 126.8, 126.83, 127.0, 127.6, 127.8, 128.3, 131.1, 131.2, 131.22, 131.6, 131.7, 139.6, 142.8, 142.9, 143.0, 143.05, 149.9, 190.6; HRMS: Calcd. for $\text{C}_{28}\text{H}_{21}\text{BrO}$ (M^+H) 453.0854; found, 453.0805.

Naphtho[2,1-b]furan-2-yl(4-(1,2,2-triphenylvinyl)phenyl)methanone (10): Yield: 0.67 g, 90%; Melting point: 232 -235 °C. IR: 3108, 3021, 1643, 1599, 1312, 807 cm^{-1} ; ^1H NMR (500 MHz, CDCl_3) δ (in ppm) 7.06 – 7.14 (m, 6H), 7.14 – 7.22 (m, 9H), 7.26 (d, $J = 10.0$ Hz, 2H), 7.59 (t, $J = 15.0$ Hz, 1H), 7.69 (t, $J = 15.0$ Hz, 1H), 7.76 (d, $J = 5.0$ Hz, 1H), 7.90 – 7.95 (m, 3H), 7.99 - 8.01 (m, 2H), 8.20 (d, $J = 10.0$ Hz, 1H); ^{13}C NMR (126 MHz, CDCl_3) δ (in ppm) 112.9, 115.2, 122.9, 123.4, 125.6, 126.8, 127.0, 127.4, 127.7, 127.9, 128.0, 128.2, 129.1, 129.1, 130.0, 130.6, 131.2, 131.3, 131.4, 131.5, 135.0, 139.9, 142.8, 143.1, 143.2, 148.9, 152.2, 154.5, 183.2; HRMS: Calcd. for $\text{C}_{39}\text{H}_{26}\text{O}_2$ (M^+H) 527.2011; found, 527.2005.

2-((6-(diethylamino)benzofuran-2-yl)(phenyl)methylene)malononitrile (GBY-7): Yield: 0.20 g, 90%; Melting point: 189°C. IR: 2984, 2868, 2209, 1624, 1534, 1382, 962, 705 cm^{-1} ; ^1H NMR (400 MHz, CDCl_3) δ (in ppm) 1.22 (t, $J = 7.1$ Hz, 6H), 3.45 (q, $J = 7.1$ Hz, 4H), 6.71 (dd, $J = 11.5, 2.6$ Hz, 2H), 6.82 (s, 1H), 7.33 (d, $J = 8.9$ Hz, 1H), 7.41 – 7.59 (m, 5H); ^{13}C NMR (101 MHz, CDCl_3) δ (in ppm) 12.5, 45.1, 92.0, 111.8, 114.9, 115.2, 117.6, 122.6, 123.6, 128.6, 129.4, 130.9, 134.0, 148.5, 150.6, 155.3, 160.7; HRMS: Calcd. for $\text{C}_{22}\text{H}_{19}\text{N}_3\text{O}$ (M^+H) 342.1606; found, 342.1574.

2-((5-(9H-carbazol-9-yl)benzofuran-2-yl)(phenyl)methylene)malononitrile (GBY-8): Yield: 0.20 g, 90%; Melting point: 199°C. IR: 3075, 2922, 2852, 2223, 1624, 1578, 1363, 974, 658 cm^{-1} ; ^1H NMR (400 MHz, CDCl_3) δ (in ppm) 7.11 (d, $J = 4.0$ Hz, 1H), 7.26 – 7.34 (m, 4H), 7.40 (t, $J = 16.0$ Hz, 2H), 7.52 – 7.61 (m, 4H), 7.62 – 7.72 (m, 2H), 7.78 (m, 1H), 7.85 (d, $J = 8.0$ Hz, 1H), 8.14 (d, $J = 8.0$ Hz, 2H); ^{13}C NMR (101 MHz, CDCl_3) δ (in ppm) 80.5, 109.3, 113.2, 113.5, 113.9, 119.8, 120.2, 120.4, 121.3, 123.3, 126.0, 128.4, 129.0, 129.1, 129.4, 132.0, 132.9, 134.4, 141.0, 152.0, 155.3, 157.5; HRMS: Calcd. for $\text{C}_{30}\text{H}_{17}\text{N}_3\text{O}$ (M^+) 435.1371; found, 435.1360.

2-(naphtho[2,1-b]furan-2-yl(4-(1,2,2-triphenylvinyl)phenyl)methylene)malononitrile (G3): Yield: 0.195 g, 90%; Melting point: 237°C. IR: 3074, 3020, 2219, 1628, 1602, 1340, 974, 697 cm^{-1} ; ^1H NMR (400 MHz, CDCl_3) δ (in ppm) 7.01 – 7.24 (m, 17H), 7.29 (d, $J = 8.2$ Hz, 2H), 7.37 (s, 1H), 7.58 (t, $J = 12.0$ Hz, 1H), 7.63 – 7.99 (m, 2H), 7.95 (t, $J = 20.0$ Hz, 2H), 8.06 (d, $J = 8.0$ Hz, 1H); ^{13}C NMR (100 MHz, CDCl_3) δ (in ppm); HRMS: Calcd. for $\text{C}_{42}\text{H}_{26}\text{N}_2\text{O}$ (M^+H) 574.204513; found, 575.2080.

Thermal Properties of luminogen GBY-7, GBY-8 and GBY-9

The thermal properties of luminogens **GBY-7**, **GBY-8**, **GBY-9** were analyzed using differential scanning calorimetry (DSC) and thermogravimetric analysis (TGA). DSC-TGA analysis was recorded from 35 to 600 °C at a scanning rate of 10 °C/min. DSC-TGA profiles of the synthesized luminogens **GBY-7**, **GBY-8**, **GBY-9** are as follows. All the three compounds exhibited good thermal stability showing less than 5% weight loss up to 280 °C, 330 °C and 360 °C respectively. Among all the three luminogens **GBY-9** exhibits highest melting point and well as thermal stability. Luminogens **GBY-7**, **GBY-8**, **GBY-9** exhibited melting temperatures (T_m) of 189, 199, 274 °C respectively.

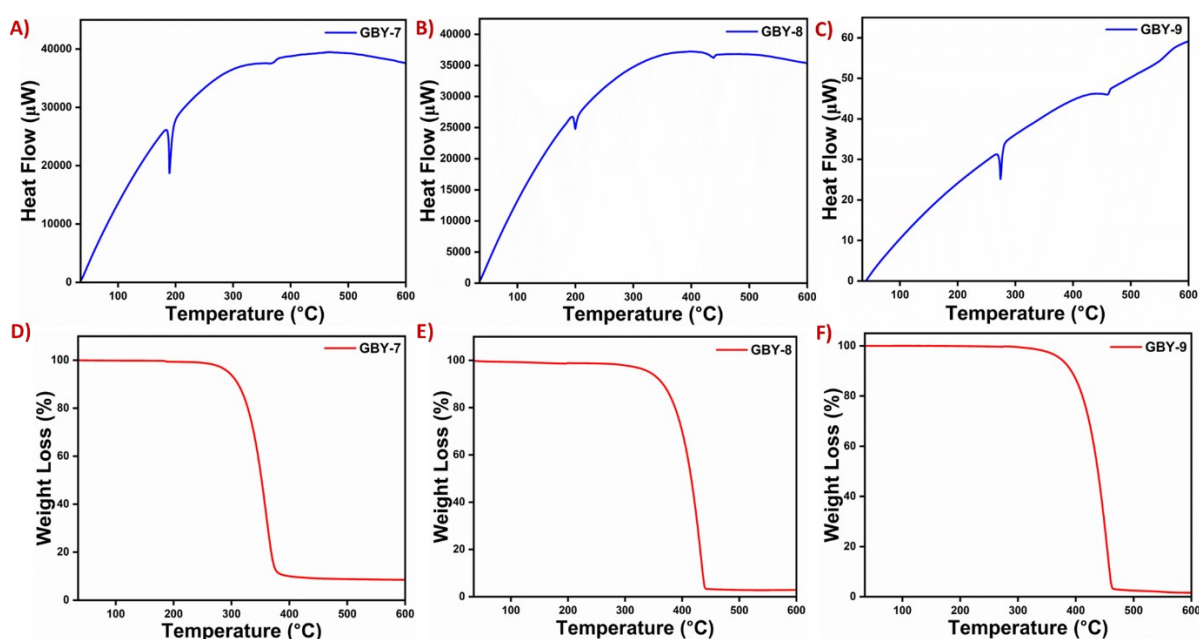


Figure S1. DSC-TGA thermograms of **GBY-7**, **GBY-8** and **GBY-9**.

Photophysical Studies

Preparation of stock solution luminogens **GBY-7**, **GBY-8** and **GBY-9** in THF solvent

Here, for **GBY-7**

Molecular weight = 341.16 g

Therefore, 341.16 g in 1000 mL of THF \equiv 1M

$$\text{Concentration (M)} = \frac{\text{Mass (g)}}{\text{Formula weight (g)} * \text{Volume (L)}}$$

Hence, to prepare 1mM stock solution 3.41 mg of **GBY-1** was dissolved in 10ml THF

Similarly, stock solution for **GBY-8**, **GBY-9** was prepared.

All the photophysical studies recorded:

Absorption maxima at molar concentration 2×10^{-5} M.

Emission maxima at molar concentration 2×10^{-5} M.

Table S1. Summary of the photophysical data in solution, aggregated state and solid state of GBY-7, GBY-8, GBY-9

Sr. No	Luminogens	Absorption Maxima (THF solvent)	Emission Maxima (THF solvent)	Emission maxima (Aggregated state)	Emission maxima (Solid state)
1	GBY-7	509	568.5	621.5	674.5
2	GBY-8	365	600.5	565	525.5
3	GBY-9	419	575.5	558.5	547

Solvatochromic properties of luminogens

Table S2. Stoke's shift calculation for GBY-7

GBY-7					
Sr. No.	Solvent	λ_{abs} (nm)	λ_{emi} (nm)	Stokes shift (nm)	Stokes shift (cm^{-1})
1	<i>n</i> -Hexane	484.5	533.5	49	1895.692426
2	Toluene	505.5	560.5	55	1941.180467
3	DCM	519	586	67	2202.97632
4	Chloroform	520.5	576	55.5	1851.184758
5	THF	509	570.5	61.5	2117.881636
6	Acetonitrile	513	596	83	2714.653898
7	DMF	521.5	600.5	79	2522.666075
8	DMSO	528.5	604	75.5	2365.184484

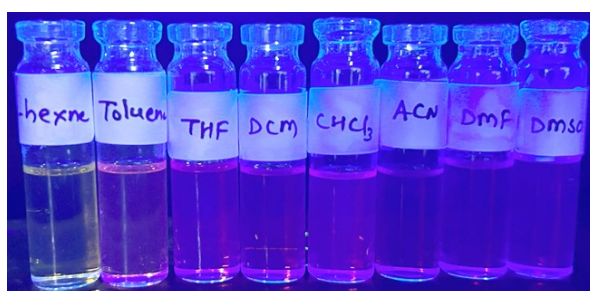


Figure S2. Effect of different solvent polarity on GBY-7 visualized under UV light (365 nm).

Table S3. Stoke's shift calculation for GBY-8

GBY-8					
Sr. No.	Solvent	λ_{abs} (nm)	λ_{emi} (nm)	Stokes shift (nm)	Stokes shift (cm^{-1})
1	<i>n</i> -Hexane	364	499.5	135.5	7452.507453
2	Toluene	372	550.5	178.5	8716.416161
3	DCM	370	406	36	2396.485155
4	Chloroform	370	591	221	10106.55325

5	THF	365	599	234	10702.76946
6	Acetonitrile	364	425	61	3943.115708
7	DMF	367.5	431	63.5	4009.028205
8	DMSO	370	432.5	62.5	3905.639744

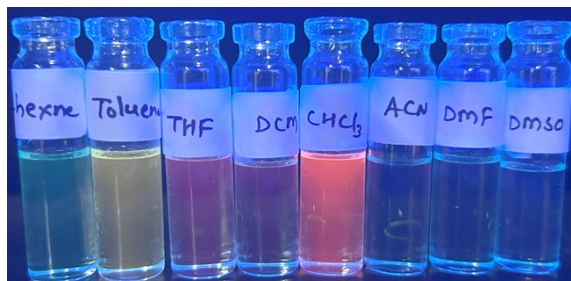


Figure S3. Effect of different solvent polarity on **GBY-8** visualized under UV light (365 nm).

Table S4. Stoke's shift calculation for **GBY-9**

GBY-9					
Sr. No.	Solvent	λ_{abs} (nm)	λ_{emi} (nm)	Stokes shift (nm)	Stokes shift (cm^{-1})
1	<i>n</i> -Hexane	413.5	515.5	102	4785.154761
2	Toluene	424.5	547	122.5	5275.590382
3	DCM	425	598	173	6807.003738
4	Chloroform	428.5	572	143.5	5854.705388
5	THF	418.5	574	155.5	6473.259817
6	Acetonitrile	417	607.5	190.5	7519.909998
7	DMF	422	618.5	196.5	7528.533717
8	DMSO	424.5	619	194.5	7402.037178

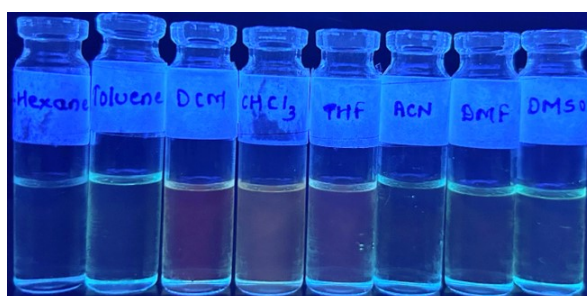


Figure S4. Effect of different solvent polarity on **GBY-9** visualized under UV light (365 nm).

Aggregation Induced Emission Studies of **GBY-7**, **GBY-8** and **GBY-9**

For UV-Visible absorption studies, the UV-visible absorption measurement was performed in a JASCO V-750 spectrophotometer under room temperature using two side opaque and two side transparent quartz cuvettes having path length equalled to 1 cm. For solution state measurement, concentration of the luminogens **GBY-7**, **GBY-8** and **GBY-9** stock was kept at 1 mM. For photoluminescence studies, the emission measurement was performed in a JASCO

FP-8200 spectrofluorimeter under room temperature using all side transparent quartz cuvette with path length equal to 1cm. Likewise absorption studies, concentration of the luminogen was kept at 1 mM throughout the solution state measurement.

Table S5. Parameter for absorption and emission.

Emission	Absorption
Excitation bandwidth = 5 nm	Bandwidth = 2 nm
Emission bandwidth = 5nm	Scan rate = 400 nm/min
Scan rate = 500 nm/min	Data interval = 0.5 nm
Data interval = 0.5 nm	Response = 0.96 nm
Sensitivity = medium	
Response = 0.1sec	

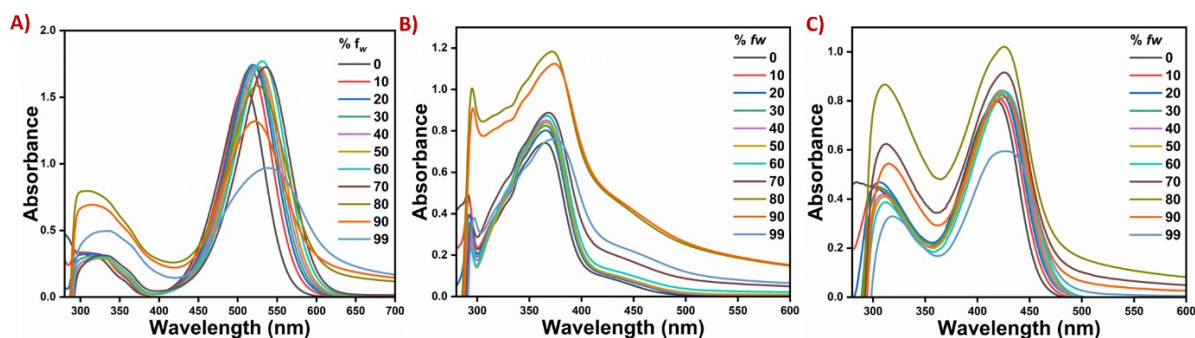


Figure S5. Uv-vis absorption spectra luminogens **GBY-7**, **GBY-8**, **GBY-9** with incremental rise in water fraction respectively.

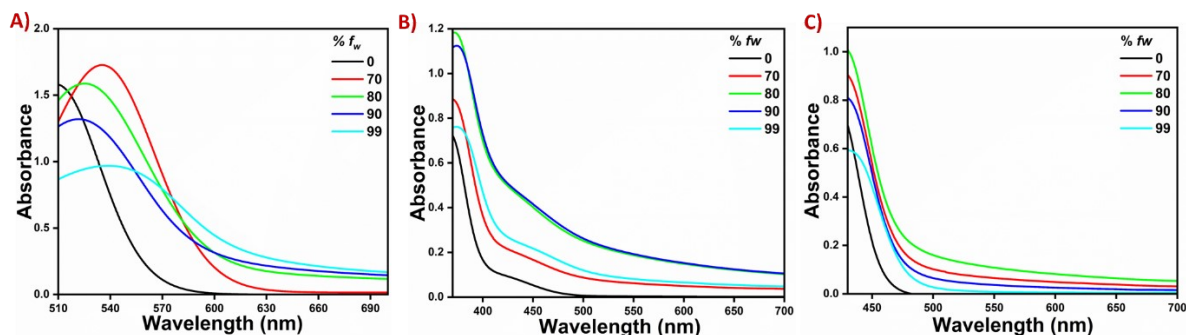


Figure S6. Absorption spectra of **GBY-7**, **GBY-8**, **GBY-9** in THF with increased f_w (%) exhibit the level of tailing in higher f_w (%) at longer wavelength region

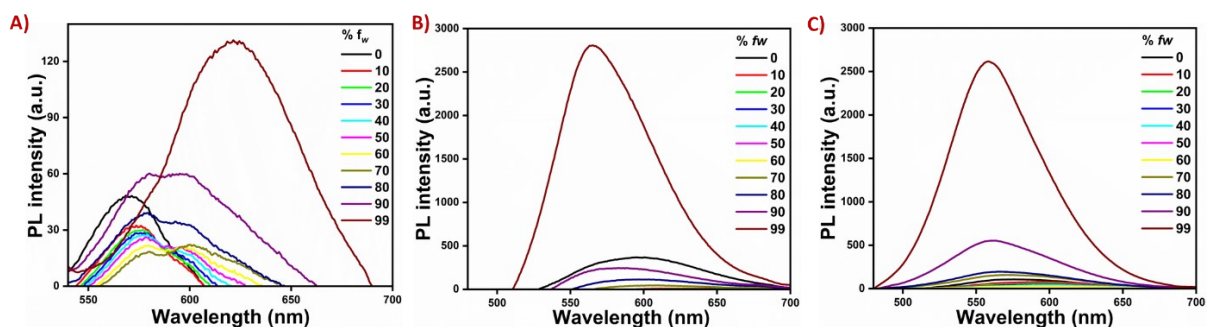


Figure S7. Emission spectra luminogens **GBY-7**, **GBY-8**, **GBY-9** with incremental rise in water fraction at excitation wavelength 311 nm, 345 nm respectively.

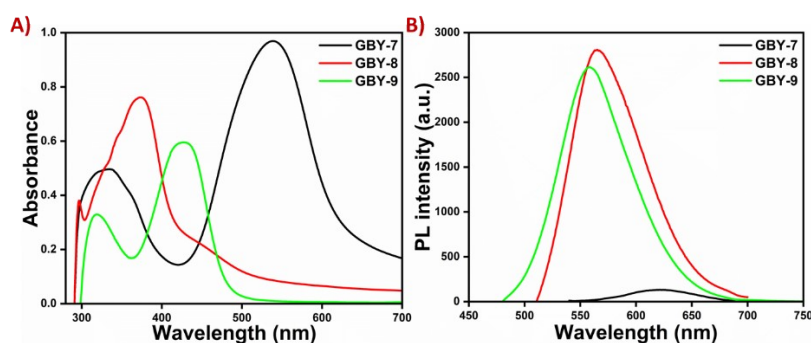


Figure S8. A) UV-vis absorption spectrum of **GBY-7**, **GBY-8** and **GBY-9** in aggregated state; B) PL spectrum of **GBY-7**, **GBY-8** and **GBY-9** in aggregated state at 2×10^{-5} M.

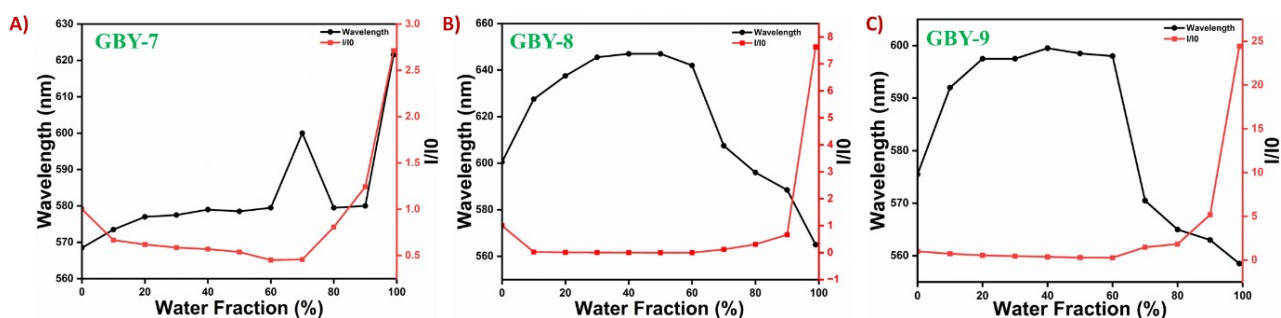


Figure S9. A), B), C) Plot of water fraction vs wavelength and relative intensity I/I_0 for **GBY-7**, **GBY-8** and **GBY-9** respectively.

Dynamic light scattering (DLS) experiments: The size distribution of the evolved aggregates in THF at higher water fraction was determined through DLS experiment, using Malvern Zetasizer Nano-ZS90 instrument. A transparent disposable polystyrene cuvette with a path length equalled to 1 cm, containing the desired solution was utilized in the experiment. A 632.8 nm red laser was employed as an excitation source at a fixed scattering angle (90° optics)

Table S6. DLS parameter of luminogens **GBY-7**, **GBY-8**, **GBY-9** in THF at water fraction (99%).

Luminogens	Z-Average (nm)	PDI	Peak 1 (Size in nm)	Peak 1 (St.Dev in nm)
GBY-7	382.6	0.148	377.7	91.96
GBY-8	279.4	0.140	246.7	69.57
GBY-9	190.6	0.146	148.2	42.05

Scanning Electron Microscopy: Scanning electron microscope (SEM) images of luminogens **GBY-7**, **GBY-8**, **GBY-9** aggregates, were recorded using SEM Quanta 200 – EDX system. Before recording the images, sonicate the sample and was placed using glass capillary on the aluminium stub. Mount sample over carbon tape whose half portion was covered with aluminium foil on aluminium stub.

Preparation of Nanoaggregates: Nanoaggregates of luminogens **GBY-7**, **GBY-8**, **GBY-9** were prepared by adding 50 μL of stock solution (0.1 mM) in a solution containing 4.95 mL of water and 0.05 mL of THF with vigorous shaking.

Tyndall Effect: The enhancement in emission intensity was attributed to the formation of aggregates, which was further validated by the Tyndall effect and DLS experiments. When a beam of light passes through a colloid, the colloidal particles present in the solution do not allow the beam to completely pass through. The light collides with the colloidal particles and is scattered (it deviates from its normal trajectory, which is a straight line). This scattering makes the path of the light beam visible. Tyndall effect^[4] was observed when laser light was passed through the aggregated states (99% water) of luminogens.

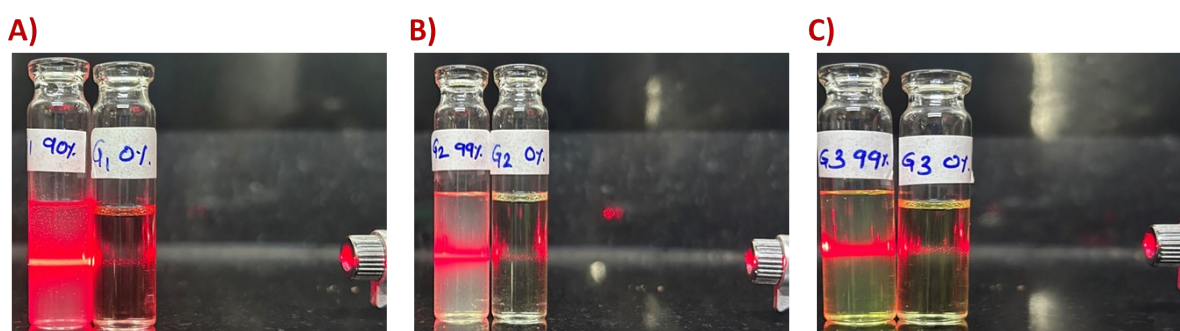


Figure S10. Tyndall effect of **GBY-7**, **GBY-8**, **GBY-9**.

Fluorescence Quantum Yield Calculation

The fluorescence quantum yield of **GBY-8** and **GBY-9** was measured in THF solvent and at their aggregated state (f_w 99% H_2O) taking quinine sulfate as the standard ($\Phi = 0.54$ in 0.1 M H_2SO_4)

$$\phi_x = \phi_{ST} * \frac{(Grad_x)}{(Grad_{ST})} * \frac{(\eta_x)^2}{(\eta_{ST})^2}$$

Here, ϕ_x = Quantum yield (**G3**)

ϕ_{ST} = Quantum yield (quinine sulphate)

η_x = Refractive index of THF

η_{ST} = Refractive index of 0.1M H₂SO₄

In order to find out gradient for **GBY-8 and GBY-9**, optical density (from UV) vs curve area (from emission) in solvent as well as in their aggregated state was plotted.

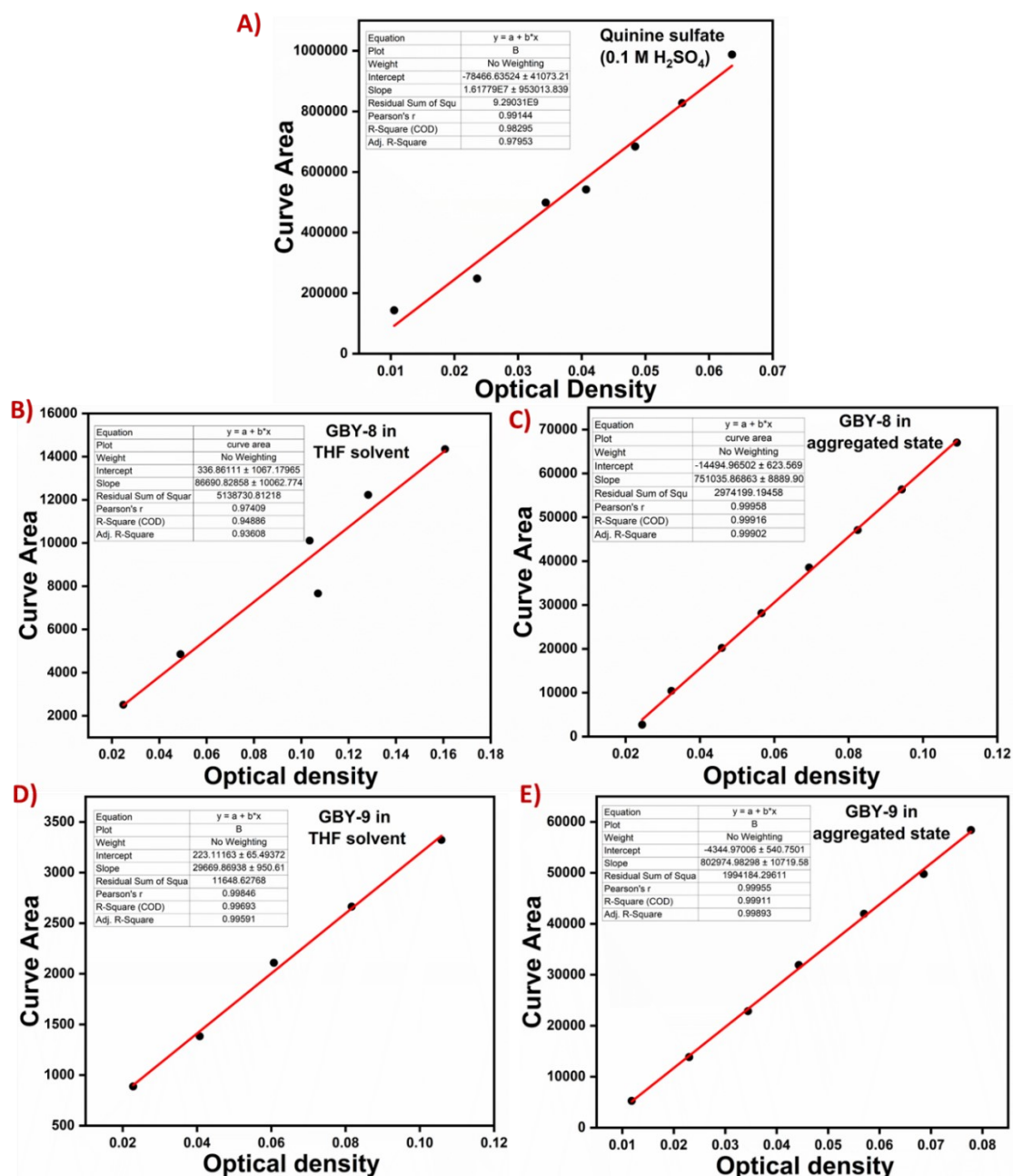


Figure S11. The plot of Integrated fluorescence intensity (Curve area) vs Optical density (Absorbance) for quinine sulphate in 0.1M H₂SO₄, **GBY-8 and GBY-9** in THF solvent as well as in aggregated state.

Table S7. Summary of the photoluminescence data of **GBY-7**, **GBY-8** and **GBY-9**.

Sr. No	Luminogens	Emission maxima in THF solvent/Aggregated state	Fluorescence Quantum yield		Solid state (%)
			0% water (Solution state)	99% water (Aggregated state)	
1	GBY-7	568.5	-	-	5.20
2	GBY-8	600.5/565	0.0032	0.0281	10.83
3	GBY-9	575.5/558.5	0.0011	0.0300	5.37

Cyclic Voltammetry Analysis and DFT study

Cyclic Voltammetry Analysis of GBY-7, GBY-8, GBY-9: The cyclic voltammetry and DFT calculation were performed to evaluate the electrochemical properties of the luminogens **GBY-7**, **GBY-8**, **GBY-9**. The redox potentials of **GBY-7**, **GBY-8**, **GBY-9** corresponding to the HOMO (highest occupied molecular orbital) energy levels are placed at -5.81, -5.94, and -5.92 respectively, and the corresponding HOMO-LUMO band gap values for **GBY-7**, **GBY-8** and **GBY-9** are 2.38, 3.36, 2.94 respectively.

The electrochemical study was carried out by cyclic voltammetry. Cyclic voltammetry measurements were recorded in an electrolyte solution of 0.1 M tetrabutylammonium hexafluorophosphate ($t\text{Bu}_4\text{NPF}_6$) in DMF using Ag/AgCl as reference electrode and platinum gauze as the counter electrode. Glassy carbon electrode was used as a working electrode and the analysis was carried out at a scan rate of 25 mV/s. The concentration of all three analyte (Luminogens) used was 1 mM. To perform the experiment, the three-electrode system was subjected to a solution containing both analyte and electrolyte in 1:1 proportion.

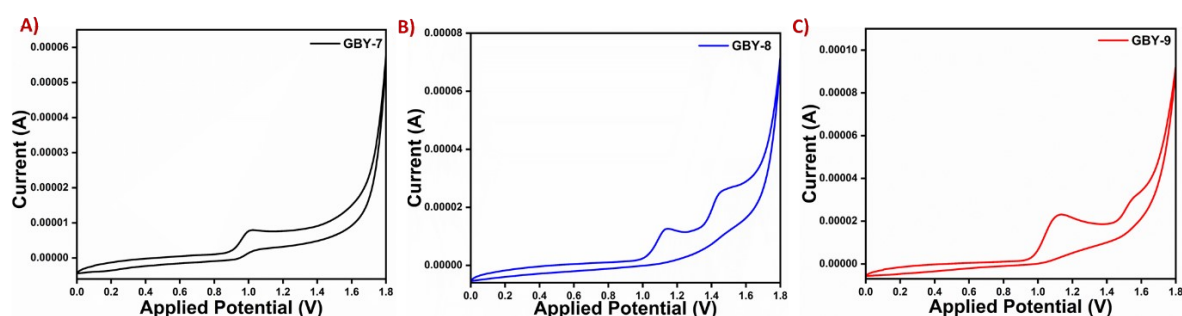


Figure S12. Cyclic voltammogram of **GBY-7**, **GBY-8** and **GBY-9**.

Bandgap Calculations of GBY-7, GBY-8 and GBY-9

HOMO and LUMO energies and HOMO-LUMO energy gap (EHL) of Luminogens **GBY-7**, **GBY-8** and **GBY-9** calculated at DFT/B3LYP/6-311++ G (d, p) level.

For **GBY-8**

Onset absorption wavelength (λ_{max}) DMF: 369 nm

Onset CV oxidation: 1.14 V and 1.45

$$\begin{aligned}
 E_{\text{HOMO}} &= -(4.8 + E_{\text{OX onset}}) \text{ eV} \\
 &= -(4.8 + 1.14) \text{ eV} \\
 &= -5.94 \text{ eV} \dots\dots\dots (\text{Corresponding to } 1.14 \text{ V}) \\
 E_{\text{HOMO}} &= -(4.8 + E_{\text{OX onset}}) \text{ eV} \\
 &= -(4.8 + 1.45) \text{ eV} \\
 &= -6.25 \text{ eV} \dots\dots\dots (\text{Corresponding to } 1.45 \text{ V}) \\
 E_{\text{band gap}} &= 1240/\lambda_{\text{max}} \\
 &= 1240/369 \\
 &= 3.36 \text{ eV} \\
 E_{\text{LUMO}} &= E_{\text{HOMO}} + E_{\text{band gap}} \\
 &= -5.94 + 3.36 \\
 &= -2.58 \text{ eV} \dots\dots\dots (\text{Corresponding to } 1.14 \text{ V}) \\
 E_{\text{LUMO}} &= E_{\text{HOMO}} + E_{\text{band gap}} \\
 &= -6.25 + 3.36 \\
 &= -2.89 \text{ eV} \dots\dots\dots (\text{Corresponding to } 1.45 \text{ V})
 \end{aligned}$$

Table S8. Electrochemical Data of GBY-7, GBY-8 and GBY-9 in DMF.

Luminogens		E (Onset/ox) [V]	λ_{onset} (nm)	HOMO [eV]	LUMO [eV]	Band gap [eV]
GBY-7	1a	1.01	521	-5.81	-3.43	2.38
GBY-8	1a	1.14	369	-5.94	-2.58	3.36
GBY-9	1a	1.12	421	-5.92	-2.98	2.94

$$\begin{aligned}
 E_{\text{HOMO}} &= -(4.8 + E_{\text{ox onset}}) \text{ eV} \\
 E_{\text{LUMO}} &= E_{\text{HOMO}} + E_{\text{band gap}} \\
 \text{Band gap} &= (E_{\text{LUMO}} - E_{\text{HOMO}}) \text{ eV or } 1240/\lambda_{\text{max onset}}
 \end{aligned}$$

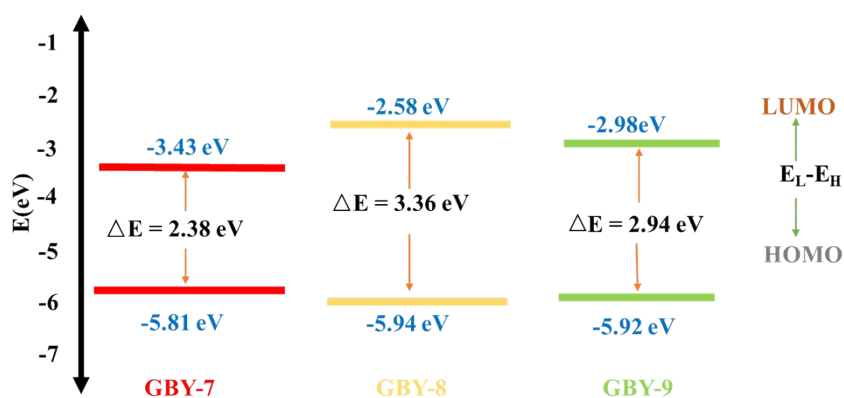


Figure S13. The experimentally calculated HOMO-LUMO energy gap of Luminogens GBY-7, GBY-8 and GBY-9 from cyclic voltammety analysis

DFT Calculations

To evaluate the theoretical bandgap of the luminogens **GBY-7**, **GBY-8** and **GBY-9** density functional theory (DFT) calculations were performed at DFT/ B3LYP level of theory using the Gaussian 09 suite of program. Energy minimization of structures was carried out at a 6-311+G(d,p) basis.^[5]

The DFT calculations showed that in **GBY-7**, the HOMO is localized at the donor (NEt₂), benzofuran, and acceptor (dicyano) moieties, while the LUMO covers the entire scaffold. In **GBY-8**, the HOMO is localized at carbazole and benzofuran, and the LUMO is distributed over the entire molecule except the carbazole part. For **GBY-9**, the HOMO is over tetraphenylethene, and the LUMO is on the naphthafuran ring and dicyano moiety. Experimentally, **GBY-7** has a smaller band gap than **GBY-8**, while **GBY-9** extended conjugation results in a smaller gap than **GBY-8**, with optimized geometries showing twisted conformations and varying dihedral angles between luminogens.

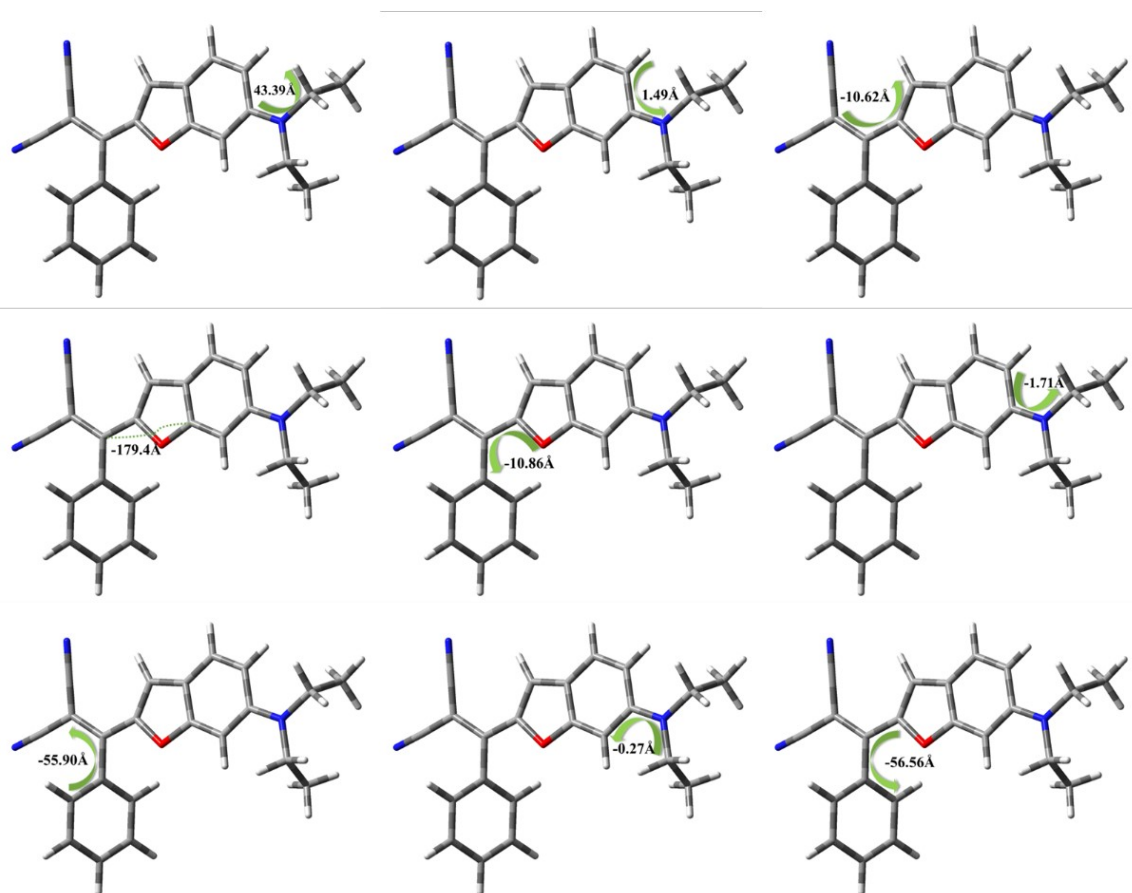


Figure S14. Dihedral angle existing between the luminogen **GBY-7**

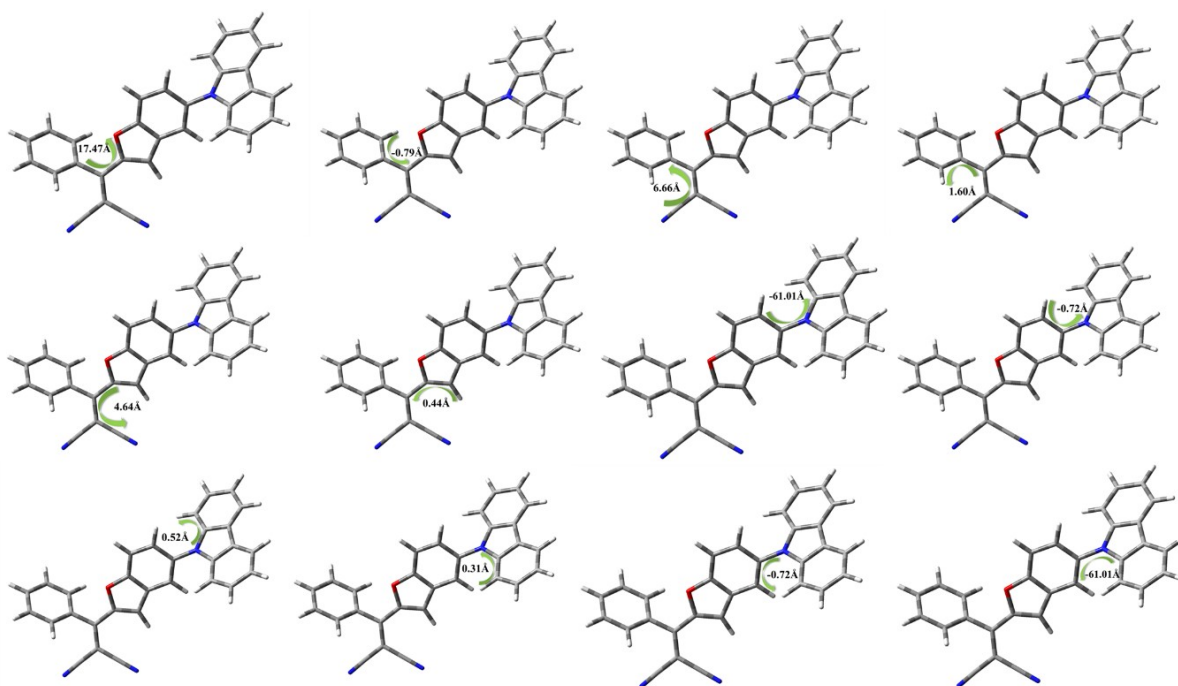


Figure S15. Dihedral angle existing within the luminogen **GBY-8**.

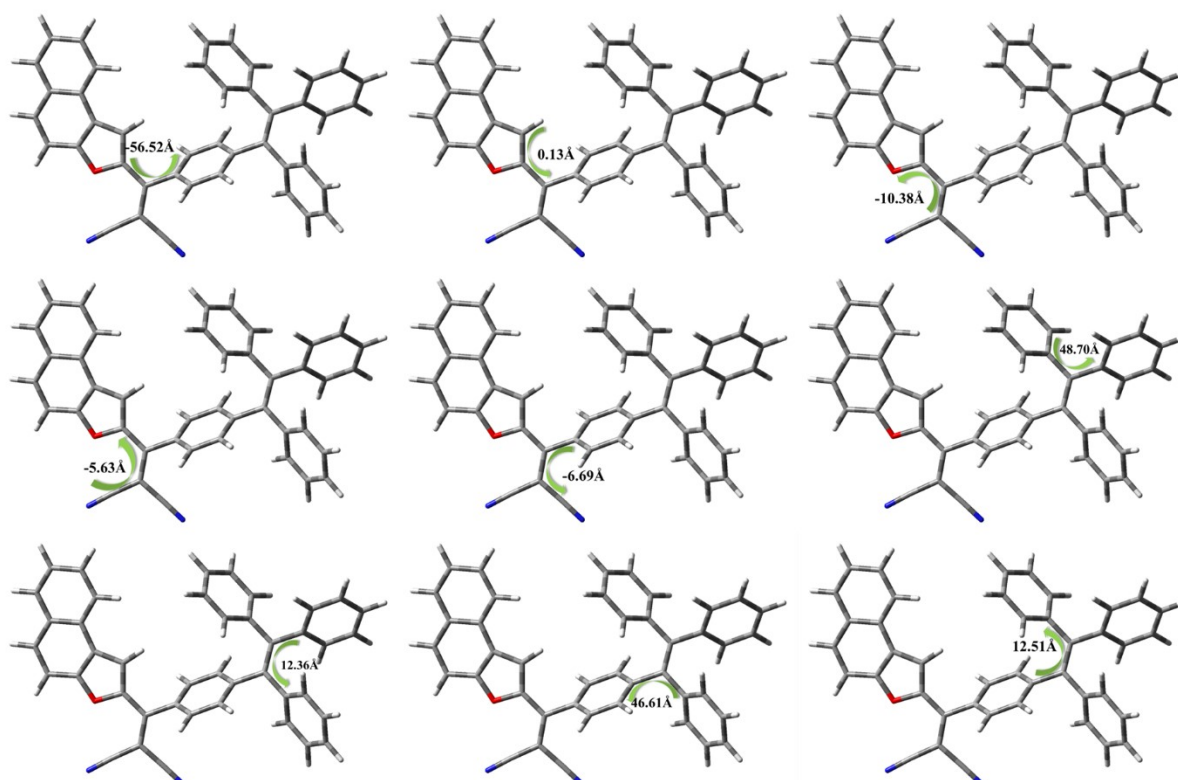


Figure S16. Dihedral angle existing within the luminogen **GBY-9**

In our current study, we focused on the geometry optimization of a given structure using the Gaussian 09 program. To achieve this, we employed the Density Functional Theory (DFT)

approach, specifically utilizing the B3LYP functional and the 6-311G basis set. Furthermore, in order to refine the energy, we performed single-point energy calculations at the B3LYP/6-311++G(d,p) level of theory. In addition to optimizing the structure and refining the energy calculations, we also investigated the impact of the solvent on the structures. To achieve this, we conducted single-point electronic structure calculations using an implicit CPCM model at the B3LYP/6-311++G(d,p) level of theory. Specifically, we considered the DMF (Dimethylformamide) solvent environment. The Cartesian coordinates for the optimized structure are provided.

Cartesian Coordinates

GBY-7

Total energy -1089.15826519 a.u.

Charge: 0

Spin: Singlet

Dipole moment: 11.5553 Debye

Function/Basis set: B3LYP/6-311G

C	-3.69149400	0.01524300	-0.13237800
C	-2.81064100	-1.09802100	-0.36151000
C	-1.41544100	-0.85335700	-0.40016400
C	-0.99067100	0.45033600	-0.23473300
C	-1.84178100	1.55463800	-0.02069400
C	-3.22750200	1.30708700	0.03080000
O	0.32963400	0.87602500	-0.24336800
C	0.30636600	2.29367700	-0.03400600
C	-1.00645100	2.70287600	0.10358300
C	1.58851300	2.93695800	-0.02227100
C	1.74658000	4.31626800	-0.05556500
C	2.80017900	2.06649100	0.02435800
C	3.79170200	2.17807200	-0.96308700
C	4.93168600	1.37515500	-0.91336700
C	5.09977500	0.45968800	0.12735500

C	4.11708700	0.34269500	1.11505200
C	2.97013800	1.13257500	1.06014000
N	-3.31978800	-2.37656600	-0.55123100
C	-4.76796100	-2.64945600	-0.48891400
C	-2.42055900	-3.51734500	-0.80485800
C	-5.33142600	-2.79658800	0.93366900
C	-1.80114600	-4.13909000	0.45759200
C	3.02524800	4.93704300	0.08155000
N	4.04907900	5.48910100	0.20000600
C	0.65516300	5.22180000	-0.19345700
N	-0.24273400	5.96382500	-0.30024500
H	-4.75465000	-0.15184900	-0.08429500
H	-0.69004800	-1.63447000	-0.54684900
H	-3.92787200	2.11415300	0.19700700
H	-1.33865300	3.70948600	0.27671800
H	3.66549900	2.88302800	-1.77266100
H	5.68568800	1.46872900	-1.68291100
H	5.98755600	-0.15691800	0.16976100
H	4.24347600	-0.36268500	1.92532300
H	2.20850900	1.03354500	1.82015300
H	-5.30551500	-1.86761600	-1.02918400
H	-4.94108300	-3.57118600	-1.04491700
H	-3.00174500	-4.27258800	-1.33492400
H	-1.63491200	-3.20206900	-1.49451700
H	-6.40935500	-2.97056900	0.89553200
H	-4.87142100	-3.63859800	1.45147900
H	-5.15320500	-1.90066900	1.52854700

H	-1.11567400	-4.94407800	0.18258100
H	-1.24320400	-3.40106200	1.03387000
H	-2.57095400	-4.55871500	1.10594100

GBY-8

Total energy -1392.81763513 a.u.

Charge: 0

Spin: Singlet

Dipole moment: 6.0138 Debye

Function/Basis set: B3LYP/6-311G

C	0.13897100	2.10141200	-0.58012800
C	-0.18633200	1.37614900	-1.75397000
C	-0.17906500	-0.01567900	-1.77504200
C	0.14307400	-0.65087800	-0.58297600
C	0.45690500	0.03643600	0.60621900
C	0.46774200	1.44173400	0.60270800
O	0.20968900	-2.01980900	-0.36569600
C	0.56841600	-2.19668700	1.00050200
C	0.72476400	-0.96776500	1.59706400
C	0.68587100	-3.57250700	1.43254900
C	0.67594300	-3.92982800	2.76732900
C	0.82261600	-4.61536600	0.37930100
C	-0.03457200	-5.72780900	0.35865000
C	0.10601300	-6.70803600	-0.62371700
C	1.10918400	-6.59532400	-1.58863700
C	1.96646400	-5.49075900	-1.57574600
C	1.81898200	-4.50122600	-0.60639500
N	0.11733800	3.52724200	-0.61890500

C	0.91807700	4.33983600	-1.44623200
C	0.59447400	5.70127100	-1.19908600
C	-0.44127200	5.71554500	-0.18195100
C	-0.71397600	4.36257800	0.15577300
C	1.90836600	3.97487000	-2.36182100
C	2.56766700	4.99610500	-3.04755300
C	2.25284500	6.34868200	-2.82371900
C	1.27139800	6.70648500	-1.90013800
C	-1.15514300	6.73957400	0.45239300
C	-2.12237800	6.40777700	1.40002100
C	-2.38594700	5.06220100	1.71446500
C	-1.68865100	4.02289000	1.09715800
C	0.92501300	-5.26976900	3.19998500
N	1.13611300	-6.34619800	3.60195400
C	0.45014400	-2.99780200	3.82493200
N	0.27402300	-2.24106300	4.69792600
H	-0.45343700	1.92828900	-2.64315600
H	-0.42457500	-0.57578100	-2.66436100
H	0.72773600	2.00674800	1.48589600
H	1.00301200	-0.78778400	2.61857100
H	-0.81800900	-5.81708500	1.09769700
H	-0.56472700	-7.55597700	-0.63256200
H	1.22154100	-7.35962700	-2.34557300
H	2.74567100	-5.40000000	-2.32011200
H	2.47882200	-3.64541700	-0.60490200
H	2.16422800	2.93870900	-2.53148500
H	3.33883000	4.74011000	-3.76189400

H	2.78190800	7.11672000	-3.37128900
H	1.03933100	7.74898700	-1.72553900
H	-0.96154400	7.77606500	0.20865900
H	-2.67897900	7.19022400	1.89755600
H	-3.14522100	4.82543600	2.44779000
H	-1.90283500	2.99190500	1.33978700

GBY-9

Total energy -1800.75074208 a.u.

Charge: 0

Spin: Singlet

Dipole moment: 9.0329 Debye

Function/Basis set: B3LYP/6-311G

C	-6.29597700	1.01738500	-3.87348700
C	-6.97341400	0.20380800	-2.98748900
C	-6.33757100	-0.29900700	-1.82216200
C	-4.96711600	0.05851300	-1.57977600
C	-4.29669400	0.89234100	-2.50576100
C	-4.94776800	1.36272200	-3.63069400
C	-7.03925700	-1.14802500	-0.90147200
C	-6.44600200	-1.65151800	0.23473300
C	-5.10946500	-1.28915800	0.45336200
C	-4.35993300	-0.46637500	-0.39326500
O	-4.33504300	-1.68729200	1.53242300
C	-3.06555700	-1.09445700	1.36135600
C	-3.06341400	-0.35013000	0.19911600
C	-2.05310600	-1.32276300	2.35470300
C	-0.68032100	-0.86309400	2.00050200

C	-2.29635200	-1.91885300	3.57758000
C	-0.04783400	-1.32586800	0.83329600
C	1.23118500	-0.89087200	0.49953700
C	1.92048200	0.03006800	1.30917800
C	1.28915400	0.47443100	2.48524700
C	0.01055600	0.04172200	2.82395800
C	3.30430400	0.48181000	0.96744100
C	3.63964500	0.92617200	-0.28131800
C	4.28239300	0.41036100	2.09768200
C	5.05652900	1.12797500	-0.71638300
C	2.61158300	1.25482000	-1.31901500
C	5.10739900	1.50421900	2.41669800
C	5.99324500	1.44186800	3.49279000
C	6.07375400	0.28467200	4.27250300
C	5.25320300	-0.80662900	3.97393500
C	4.36064000	-0.74113800	2.90328400
C	5.43828800	2.30615900	-1.38507100
C	6.75349200	2.49303300	-1.81246200
C	7.71047400	1.49686100	-1.59887200
C	7.34061900	0.31276600	-0.95495700
C	6.02844600	0.13068600	-0.51735600
C	1.53440300	2.11188800	-1.02978300
C	0.59726000	2.44134100	-2.01091200
C	0.71535100	1.91668300	-3.30129100
C	1.78646800	1.07121100	-3.60610800
C	2.73026300	0.75342400	-2.62884300
C	-1.22427700	-2.22932100	4.47342300

N	-0.37454000	-2.51285000	5.22396000
C	-3.58895800	-2.29060700	4.06282200
N	-4.61446000	-2.60308200	4.52627100
H	-6.79497100	1.39201900	-4.75684100
H	-8.00618000	-0.06309100	-3.17316400
H	-3.26282400	1.15800300	-2.32835600
H	-4.42386500	1.99888000	-4.33138800
H	-8.07049600	-1.39283600	-1.11948100
H	-6.96847800	-2.28803100	0.93217100
H	-2.22793000	0.21787100	-0.16759500
H	-0.54993800	-2.04566700	0.20146700
H	1.70703000	-1.27091000	-0.39277600
H	1.80583700	1.16663000	3.13528300
H	-0.45856100	0.41360400	3.72407900
H	5.04936100	2.40306200	1.81914600
H	6.61572400	2.29612300	3.72433100
H	6.76044600	0.23691500	5.10708600
H	5.30190900	-1.70363800	4.57677700
H	3.71959000	-1.58557500	2.68887100
H	4.70052600	3.07660000	-1.56481700
H	7.02941300	3.41135000	-2.31402300
H	8.72884200	1.63871500	-1.93539000
H	8.07156400	-0.46890600	-0.79533600
H	5.75017200	-0.78769000	-0.02011100
H	1.44097500	2.52534400	-0.03525300
H	-0.21462900	3.11603900	-1.77136200
H	-0.00859200	2.17384500	-4.06319700

H 1.89005800 0.66628900 -4.60417600

H 3.56554700 0.11205500 -2.87585600

Hydrazine sensing

Preparation of analyte stock solution: Different amines such as pyridine, triethylamine, aniline, piperidine, diethylamine, dimethylamine, in THF solvent and thiourea, hydroxylamine hydrochloride, hydrazine in distilled water were used to prepare 1 mM stock solution.

For test solution, 100 μL of analyte stock solution and 100 μL of luminogens stock solution (1 mM) in 4.95 mL water and 50 μL THF were used to record the PL spectra.

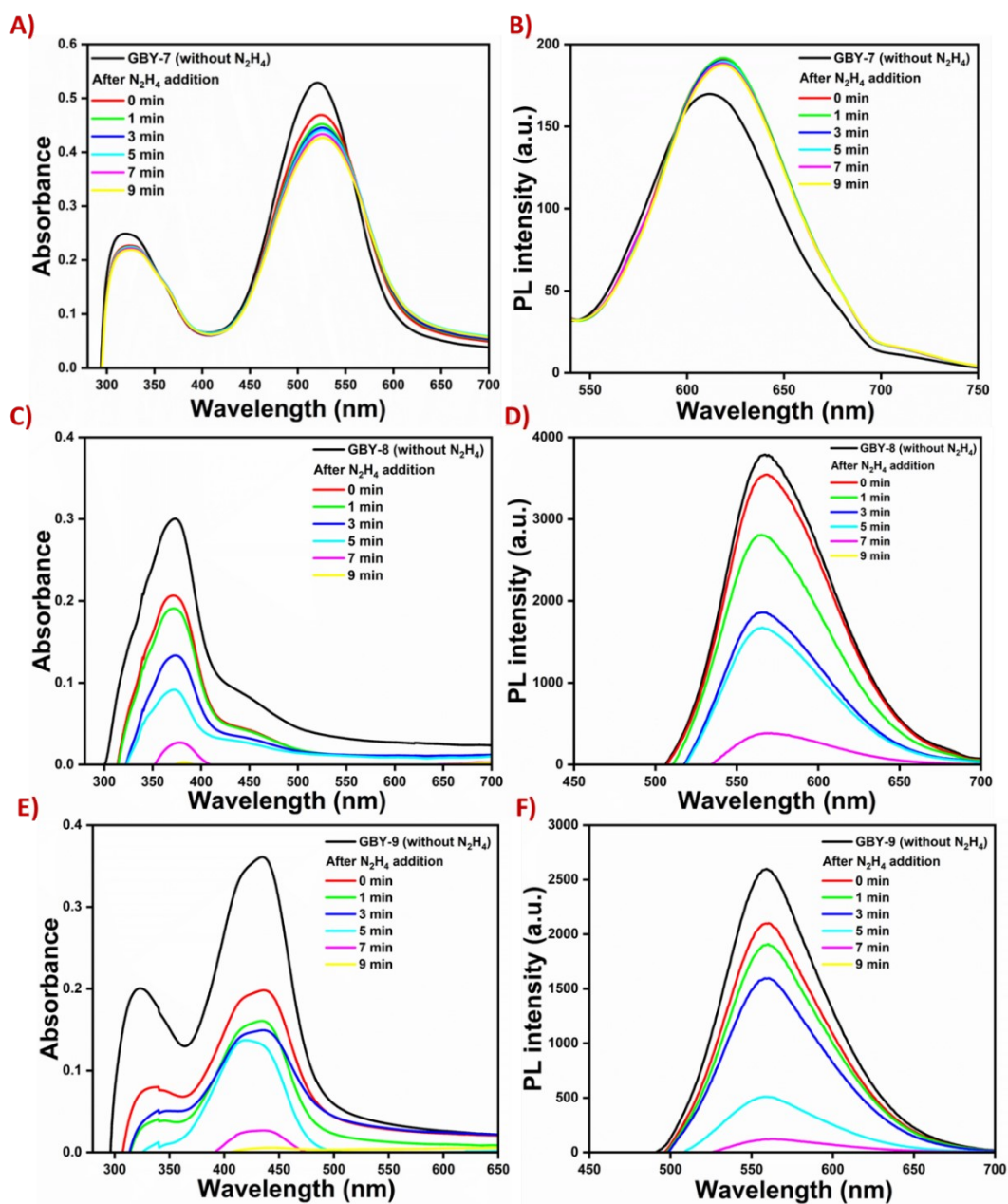


Figure S17. Time-dependent absorption and emission spectra of GBY-7, GBY-8 and GBY-9 after the addition of hydrazine.

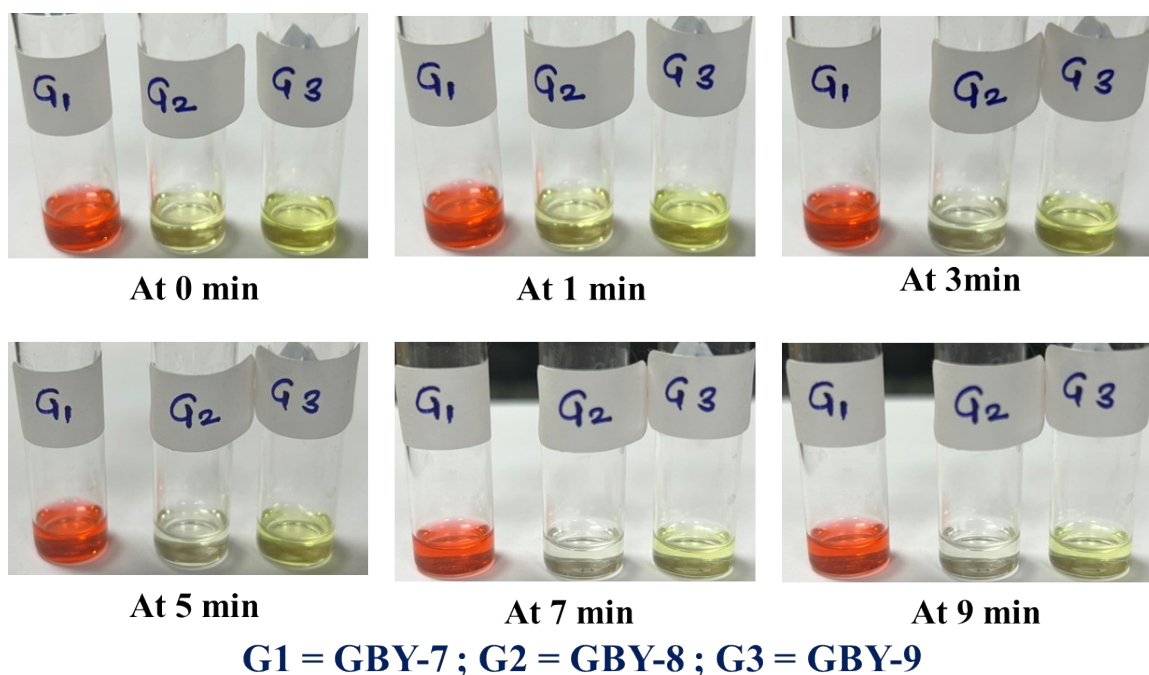


Figure S18. Visual color change of luminogens **GBY-7**, **GBY-8** and **GBY-9** in presence of hydrazine.

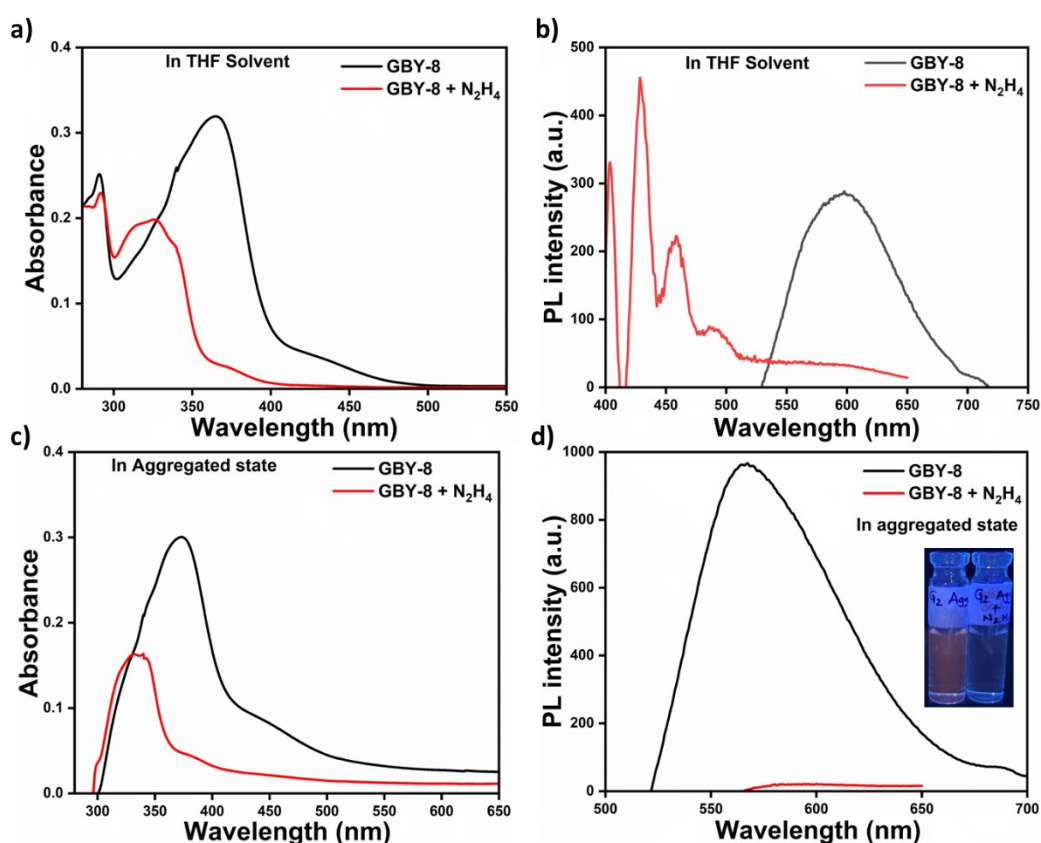


Figure S19. Absorption and emission spectra of the luminogen (**GBY-8**) in the presence as well as the absence of hydrazine in the solution state (1 mM concentration in THF solvent) as well in the aggregated state (with 99% water fraction)

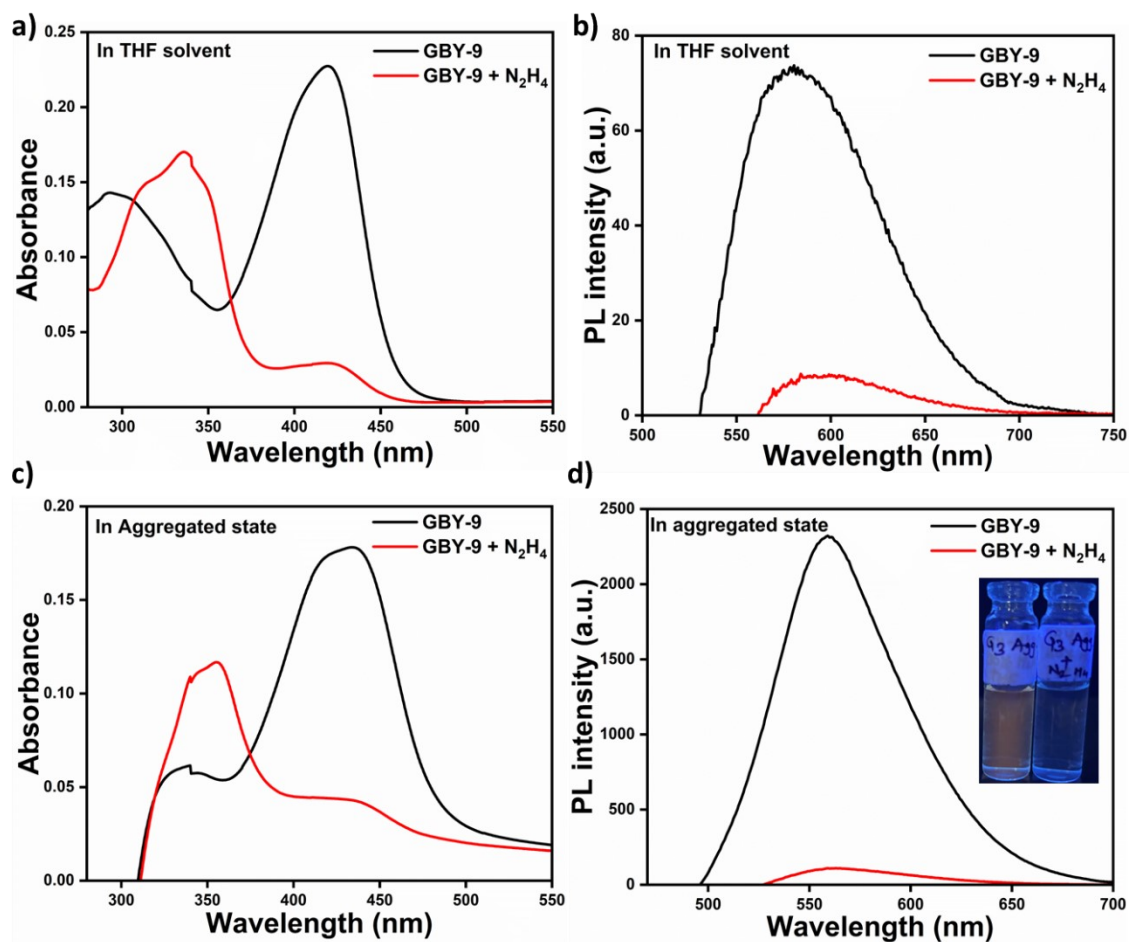


Figure S20. Absorption and emission spectra of the luminogen (GBY-9) in the presence as well as the absence of hydrazine in the solution state (1 mM concentration in THF solvent) as well in the aggregated state (with 99% water fraction)

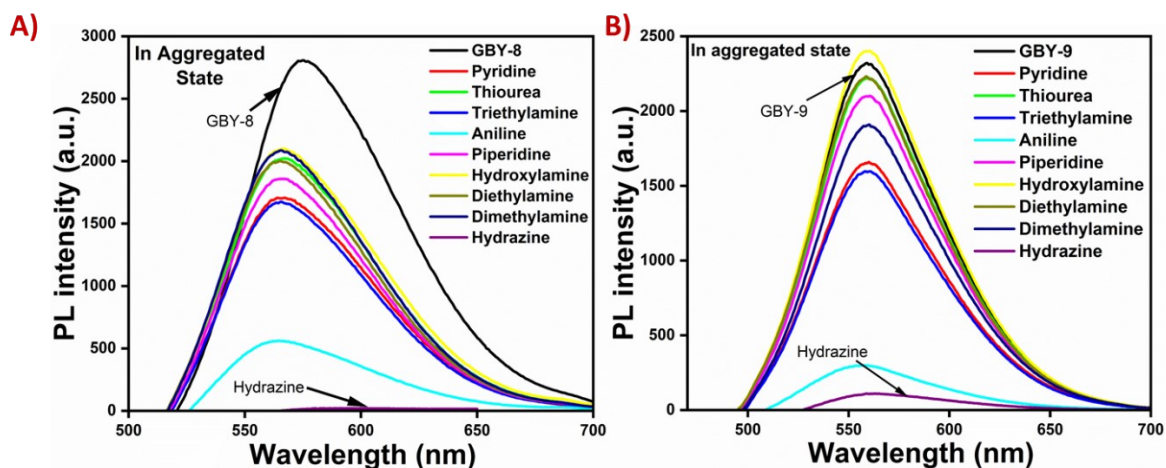


Figure S21. Selective sensing of hydrazine over other amines by GBY-8 and GBY-9 in aqueous medium.

Limit of detection

Detection limit calculations for **GBY-8** (1 mM) in THF with N_2H_4 (0 to 0.028 mM) in THF:Water (0.05:9.95 v/v)

σ = Standard Deviation obtained from 10 blank emission measurement of THF:Water (0.05:9.95 v/v)

$$\sigma = 0.4744$$

and k is slope obtained from Plot of emission intensity of **GBY-8** in THF:Water (0.05:9.95 v/v) at 371 nm versus concentration of N_2H_4 in THF

$$k = 6908.6$$

$$\text{Detection limit} = 3\sigma/k$$

$$\text{Detection limit} = 3 \times 0.4744 / 6908.6$$

$$\text{Detection limit} = 0.000206 \text{ mM}$$

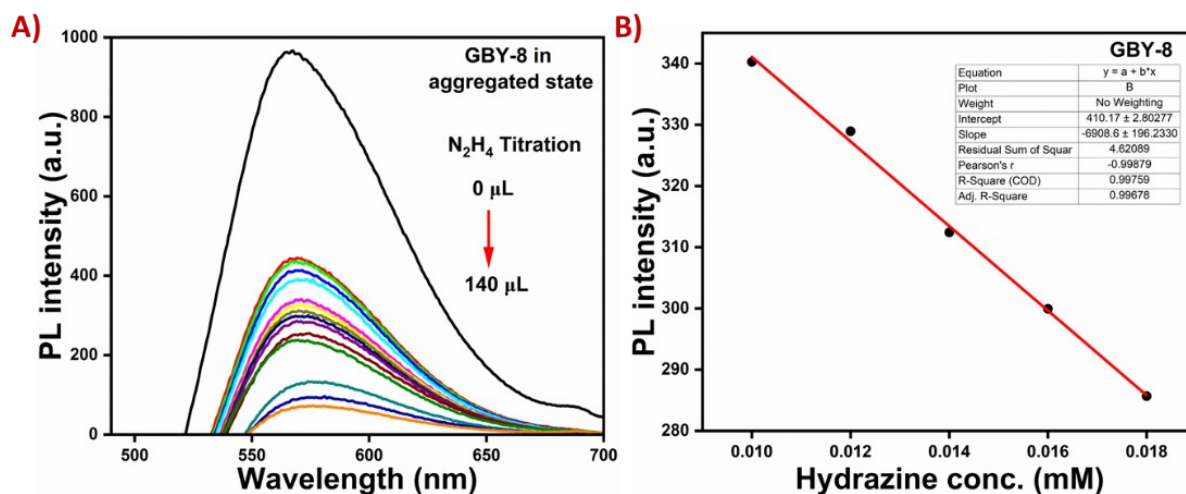


Figure S22. A) Titration of hydrazine with **GBY-8** in aggregated state; B) Plot of hydrazine concentration vs PL intensity

Detection limit calculations for **GBY-9** (1 mM) in THF with N_2H_4 (0 to 0.028 mM) in THF:Water (0.05:9.95 v/v)

σ = Standard Deviation obtained from 10 blank emission measurement of THF:Water (0.05:9.95 v/v)

$$\sigma = 21.26336$$

and k is slope obtained from Plot of emission intensity of **GBY-9** in THF:Water (0.05:9.95 v/v) at 431 nm versus concentration of N_2H_4 in THF

$$k = 14634.4$$

$$\text{Detection limit} = 3\sigma/k$$

$$\text{Detection limit} = 3 * 21.26336 / 14634.4$$

$$\text{Detection limit} = 0.0043 \text{ mM}$$

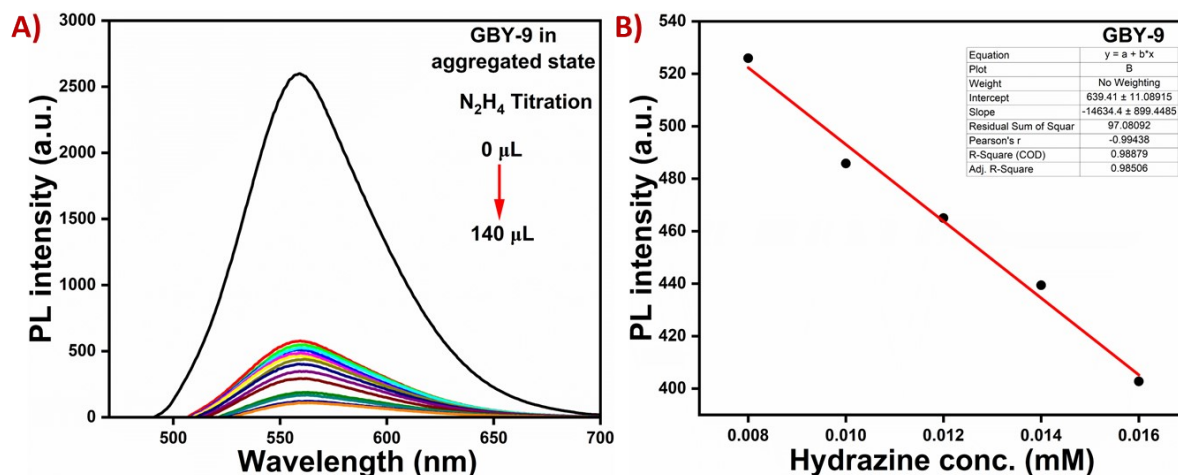


Figure S23. A) Titration of hydrazine with **GBY-9** in aggregated state; B) Plot of hydrazine concentration vs PL intensity

References:

1. Y. Lin, X. Jiang, S. T. Kim, S. B. Alahakoon, X. Hou, Z. Zhang, C. M. Thompson, R. A. Smaldone and C. Ke, An Elastic Hydrogen-Bonded Cross-Linked Organic Framework for Effective Iodine Capture in Water, *J. Am. Chem. Soc.*, 2017, **139**, 21, 7172–7175. DOI: [10.1021/jacs.7b03204](https://doi.org/10.1021/jacs.7b03204)
2. (a) V. Mahendran, K. Pasumpon, S. Thimmarayaperumal, P. Thilagar and S. Shanmugam, Tetraphenylethene–2-Pyrene Conjugate: Aggregation-Induced Emission Study and Explosives Sensor, *J. Org. Chem.* 2016, **81**, 9, 3597–3602. DOI: [10.1021/acs.joc.6b00267](https://doi.org/10.1021/acs.joc.6b00267); (b) H. Gao, D. Xu, X. Liu, A. Han, L. Zhou, C. Zhang, Z. Li and J. Dang, Tetraphenylethene-based β -diketonate boron complex: Efficient aggregation-induced emission and high contrast mechanofluorochromism, *Dyes Pigm.*, 2017, **139**, 157–165. DOI: [/10.1016/j.dyepig.2016.12.004](https://doi.org/10.1016/j.dyepig.2016.12.004)
3. (a) Z. Lu, Y. Liu, S. Lu, Y. Li, X. Liu, Y. Qin and L. Zheng, A highly selective TPE-based AIE fluorescent probe is developed for the detection of Ag⁺, *RSC Adv.*, 2018, **8**, 19701–19706. (b) G. Yashwantrao, P. Shetty, P. J. Maleikal, P. Badani, S. Saha, Dehydrative Substitution Reaction in Water for the Preparation of Unsymmetrically Substituted Triarylmethanes: Synthesis, Aggregation-Enhanced Emission, and Mechanofluorochromism, *ChemPlusChem*, 2022, **87**, 7, e202200150. (c) V.P. Jejurkar, G. Yashwantrao, P.K. Reddy, A.P. Ware, S.S. Pingale, R. Srivastava and S. Saha, Rationally Designed Furocarbazoles as Multifunctional Aggregation Induced Emissive

Luminogens for the Sensing of Trinitrophenol (TNP) and Cell-imaging, *ChemPhotoChem.*, 2020, **4**, 691-703

4. M. J. Frisch, G. W. Trucks, H. B. Schlegel, G. E. Scuseria, M. A. Robb, J. R. Cheeseman, G. Scalmani, V. Barone, B. Mennucci, G. A. Petersson, H. Nakatsuji, M. Caricato, X. Li, H. P. Hratchian, A. F. Izmaylov, J. Bloino, G. Zheng, J. L. Sonnenberg, M. Hada, M. Ehara, K. Toyota, R. Fukuda, J. Hasegawa, M. Ishida, T. Nakajima, Y. Honda, O. Kitao, H. Nakai, T. Vreven, J.A. Montgomery Jr., J. E. Peralta, F. Ogliaro, M. Bearpark, J. J. Heyd, E. Brothers, K.N. Kudin, V. N. Staroverov, R. Kobayashi, J. Normand, K. Raghavachari, A. Rendell, J.C. Burant, S.S. Iyengar, J. Tomasi, M. Cossi, N. Rega, J. M. Millam, M. Klene, J.E. Knox, J.B. Cross, V. Bakken, C. Adamo, J. Jaramillo, R. Gomperts, R. E. Stratmann, O. Yazyev, A. J. Austin, R. Cammi, C. Pomelli, J. W. Ochterski, R. L. Martin, K. Morokuma, V. G. Zakrzewski, G. A. Voth, P. Salvador, J. J. Dannenberg, S. Dapprich, A. D. Daniels, O. Farkas, J. B. Foresman, J. V. Ortiz, J. Cioslowski and D. J. Fox, *Gaussian 16, Revision A. 03*, Gaussian, Inc., Wallingford CT, **2016**.

^1H and ^{13}C NMR Spectral Reproductions Of 8, 10, GBY-7, GBY-8 and GBY-9

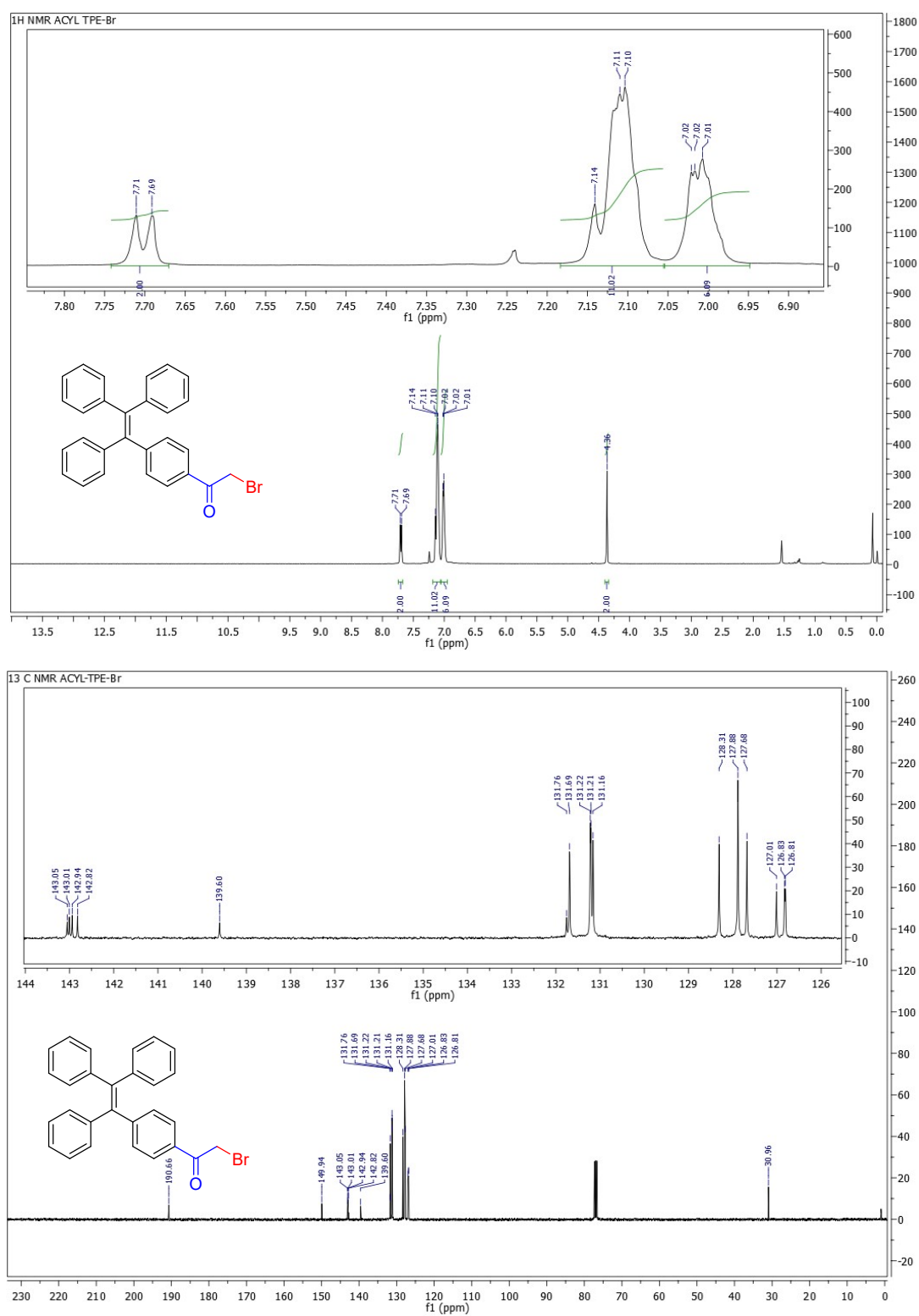


Figure 24. ^1H (400 MHz, CDCl_3) and ^{13}C NMR (100 MHz, CDCl_3) spectral reproduction of 2-bromo-1-(4-(1,2,2-triphenylvinyl)phenyl)ethan-1-one (**8**).

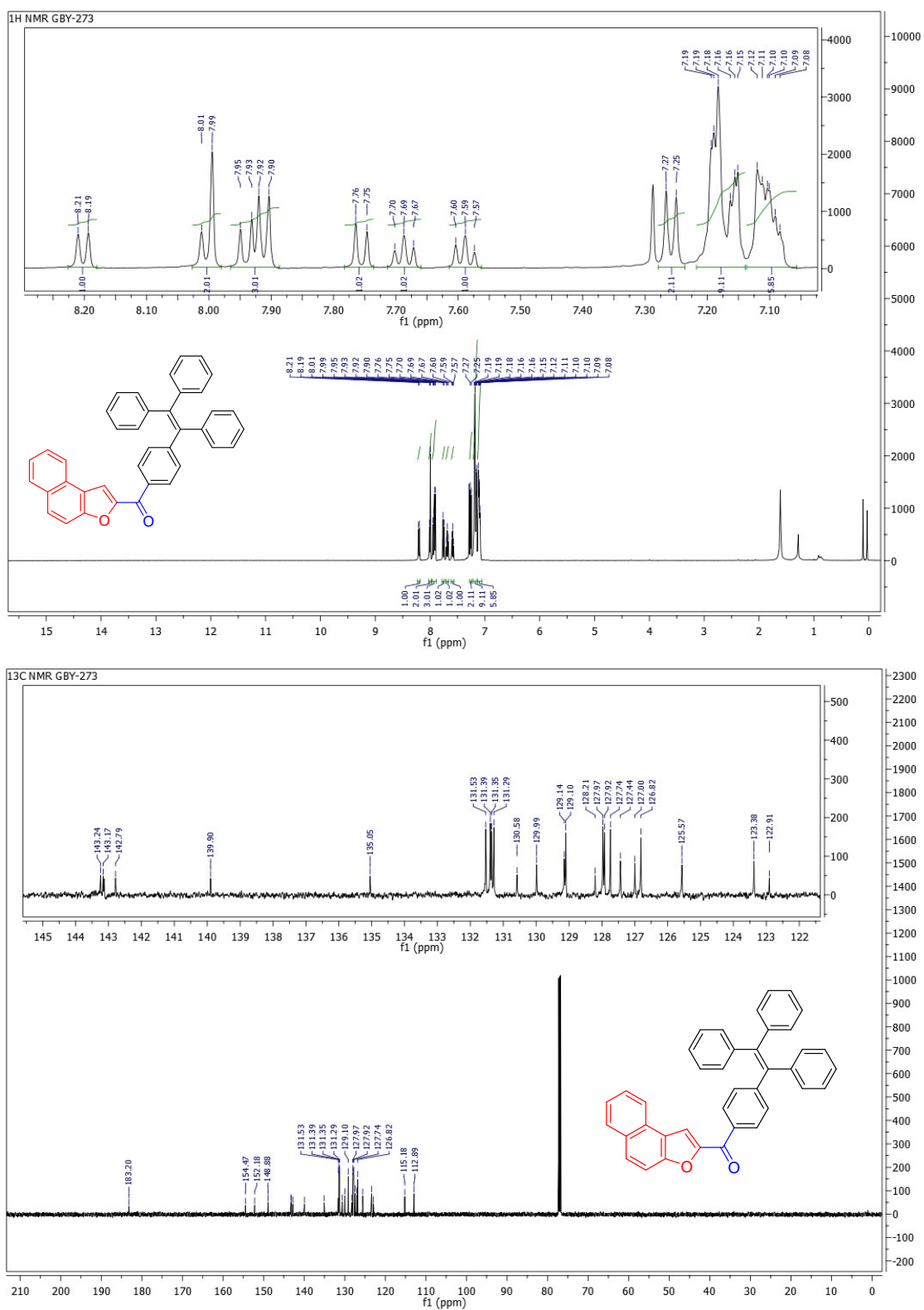


Figure 25. ¹H NMR (500 MHz, CDCl₃) and ¹³C NMR (126 MHz, CDCl₃) spectral reproduction of naphtho[2,1-b]furan-2-yl(4-(1,2,2-triphenylvinyl)phenyl)methanone (**10**).

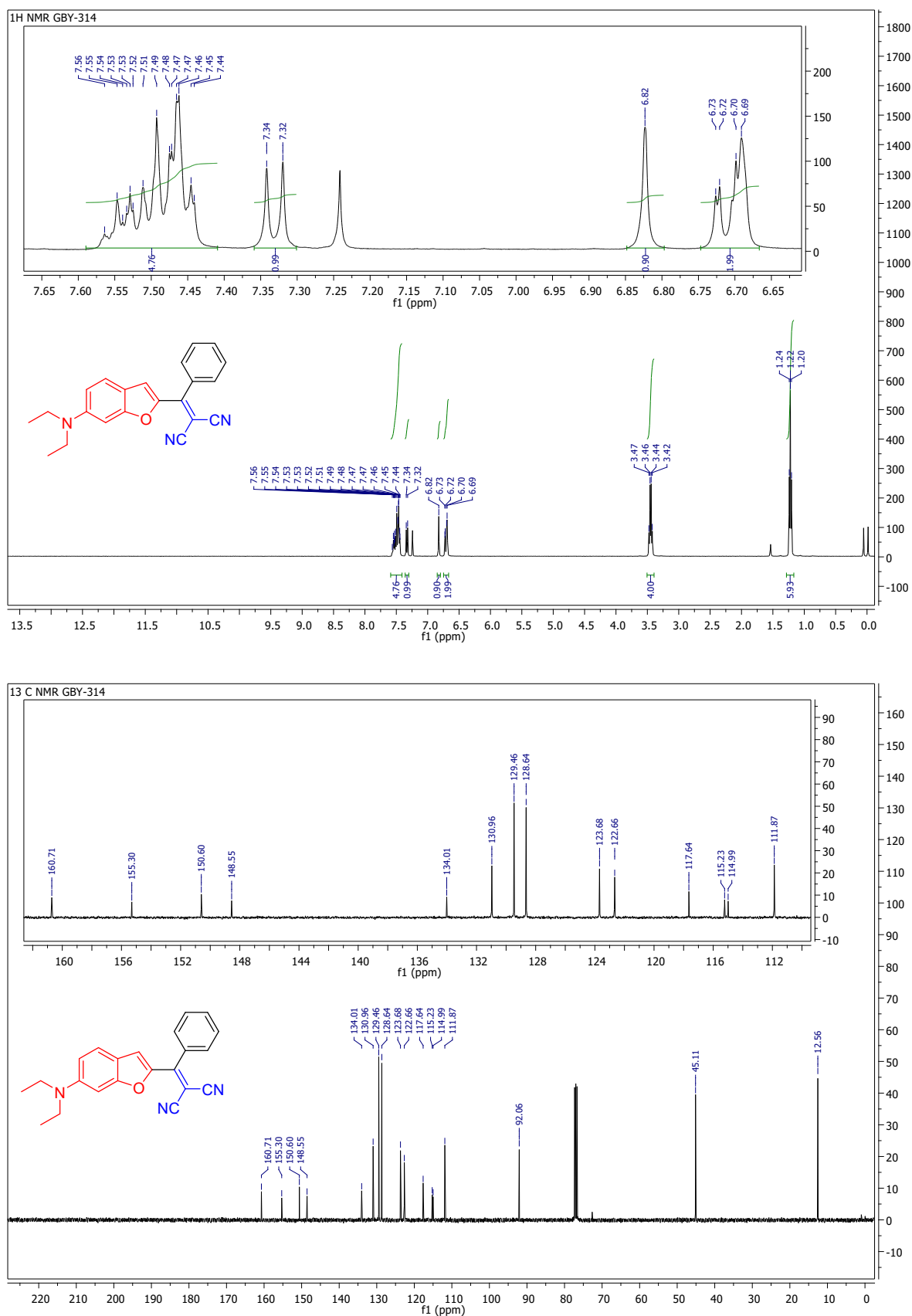
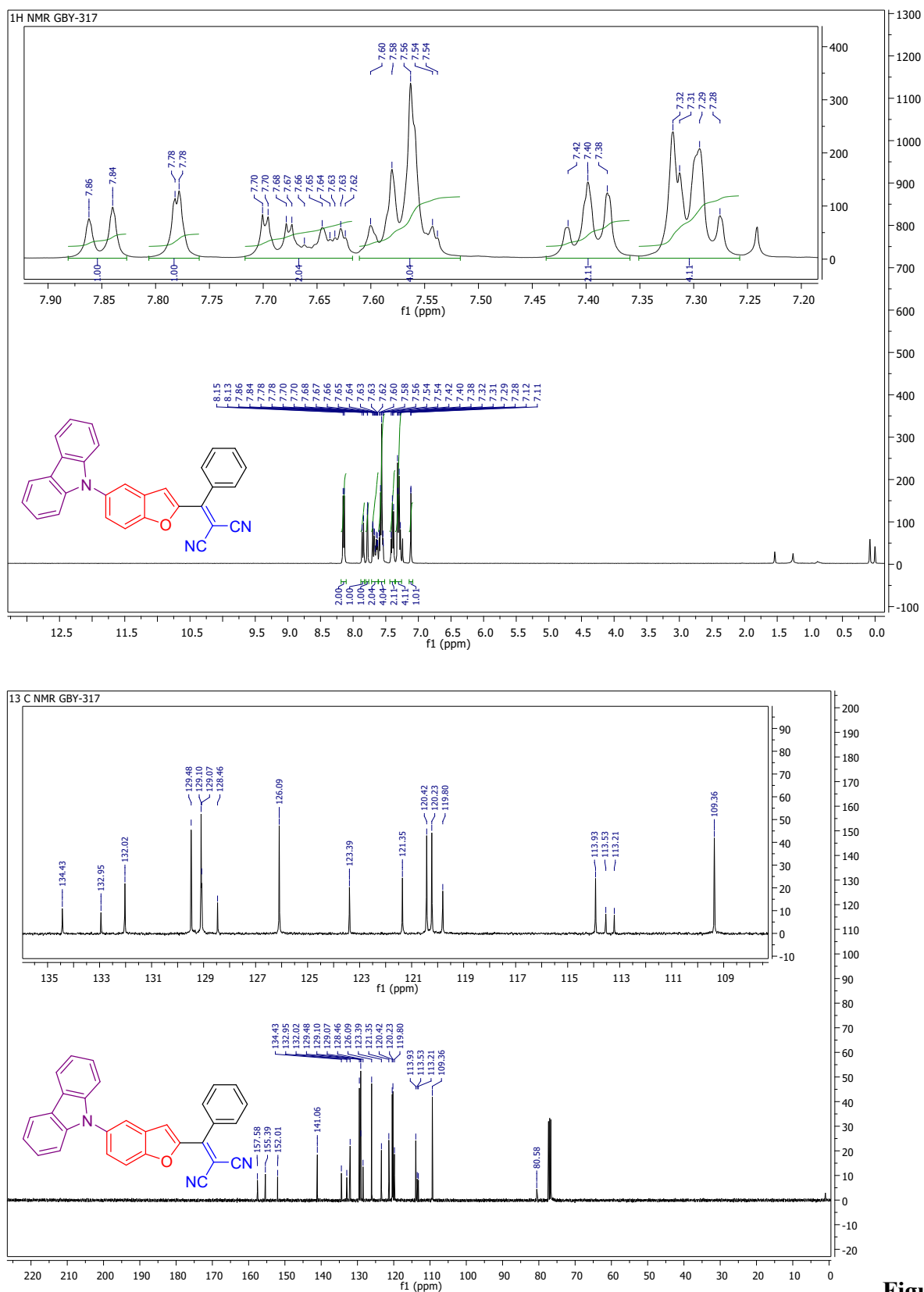


Figure 26. ¹H NMR (500 MHz, CDCl₃) and ¹³C NMR (126 MHz, CDCl₃) spectral reproduction of 2-((6-(diethylamino)benzofuran-2-yl)(phenyl)methylene)malononitrile (**GBY-7**).



re 27. ^1H NMR (500 MHz, CDCl_3) and ^{13}C NMR (126 MHz, CDCl_3) spectral reproduction of 2-((5-(9H-carbazol-9-yl)benzofuran-2-yl)(phenyl)methylene)malononitrile (**GBY-8**).

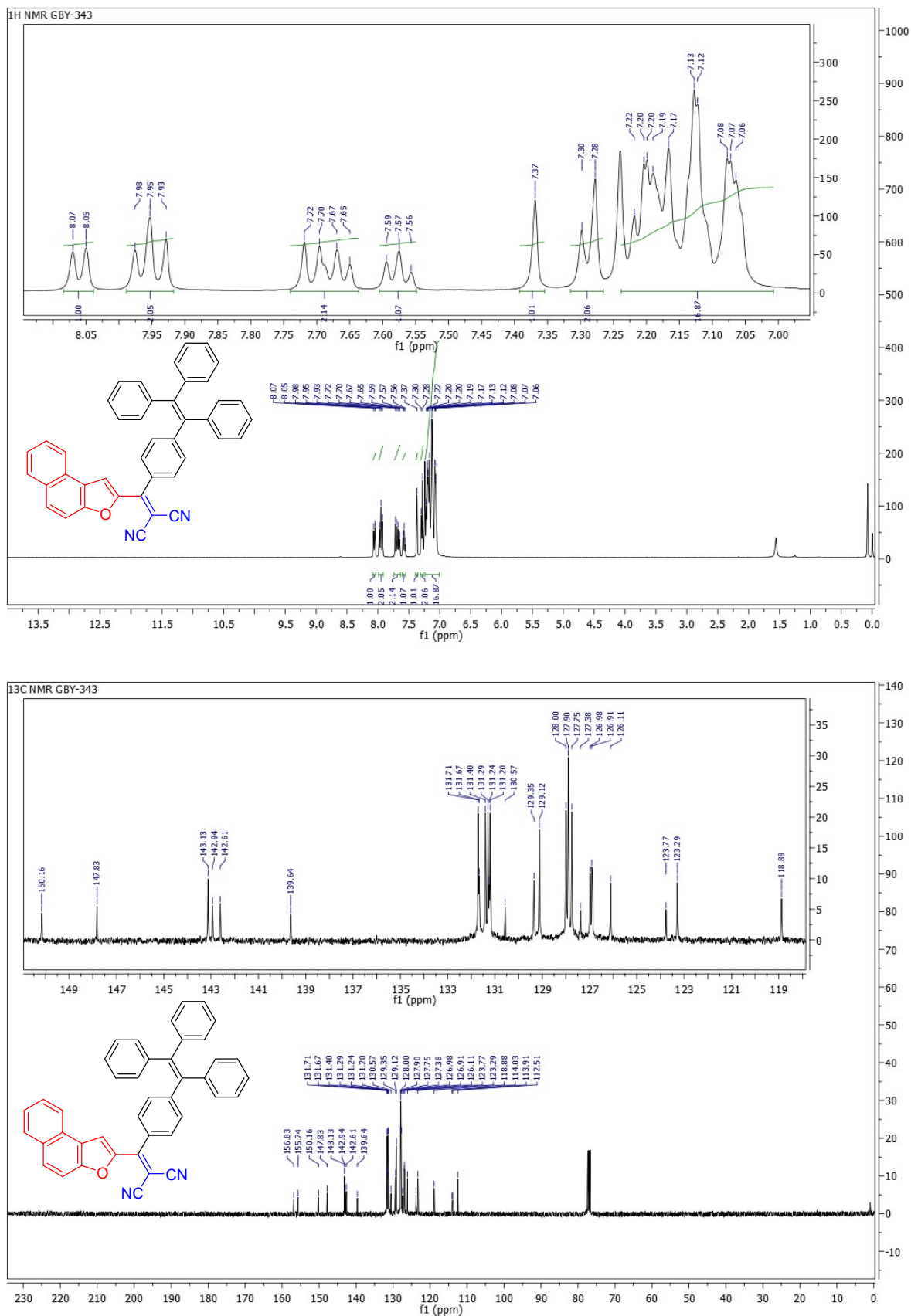


Figure 28. ^1H NMR (400 MHz, CDCl_3) and ^{13}C NMR (100 MHz, CDCl_3) spectral reproduction of (1-phenylnaphtho[2,1-b]furan-2-yl)(4-(1,2,2-triphenylvinyl)phenyl)methanone (**GBY-9**)

LC-HRMS data of 8, 10, GBY-7, GBY-8 and GBY-9

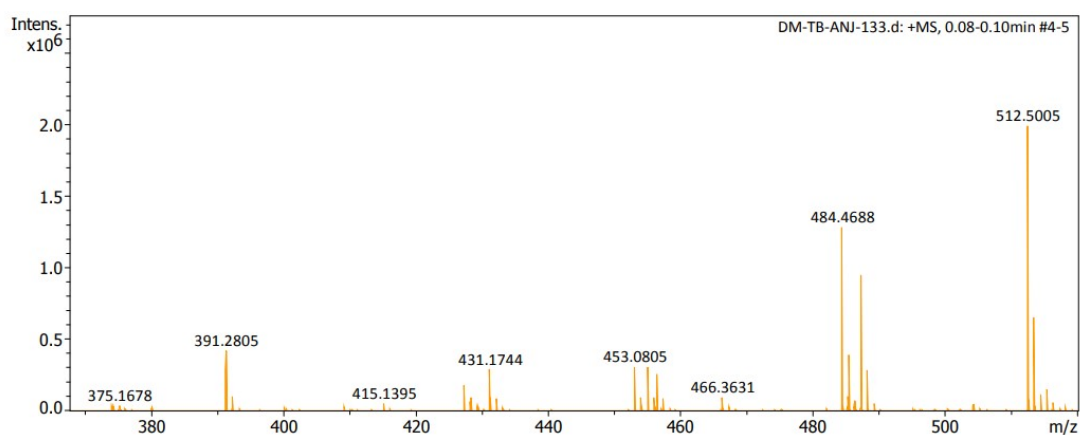


Figure S29. HR-LC-MS spectra of 8.

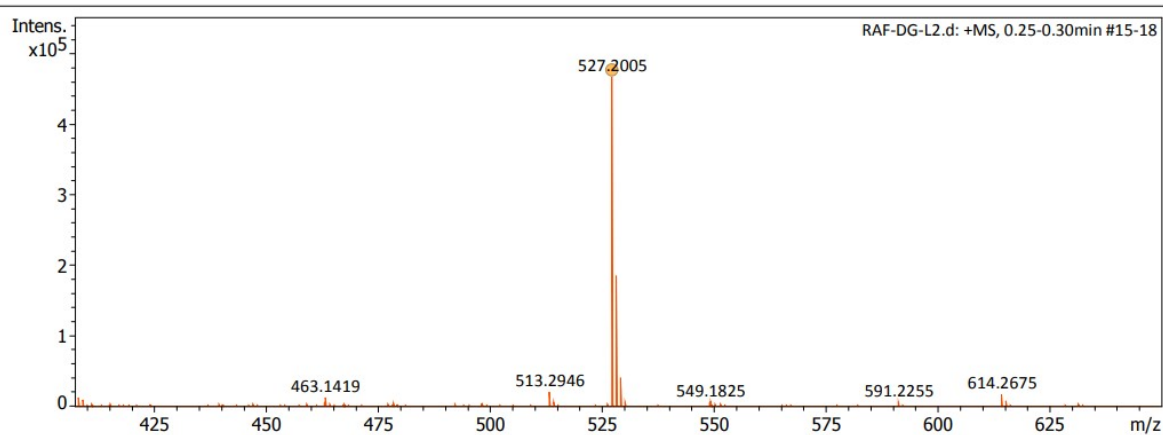


Figure S30. HR-LC-MS spectra of 10.

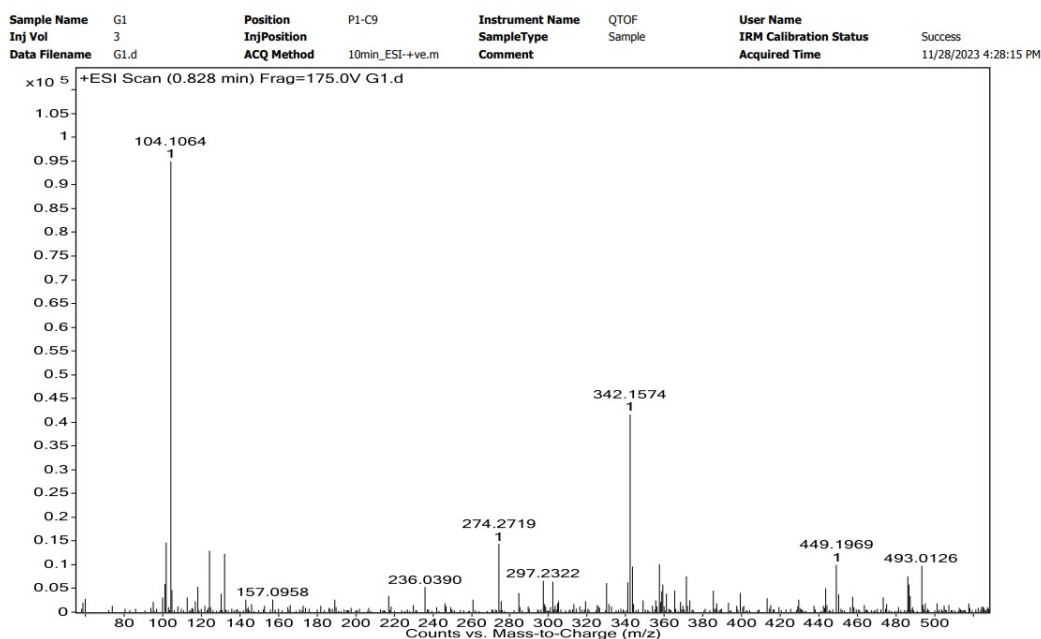


Figure S31. HR-LC-MS spectra of GBY-7.

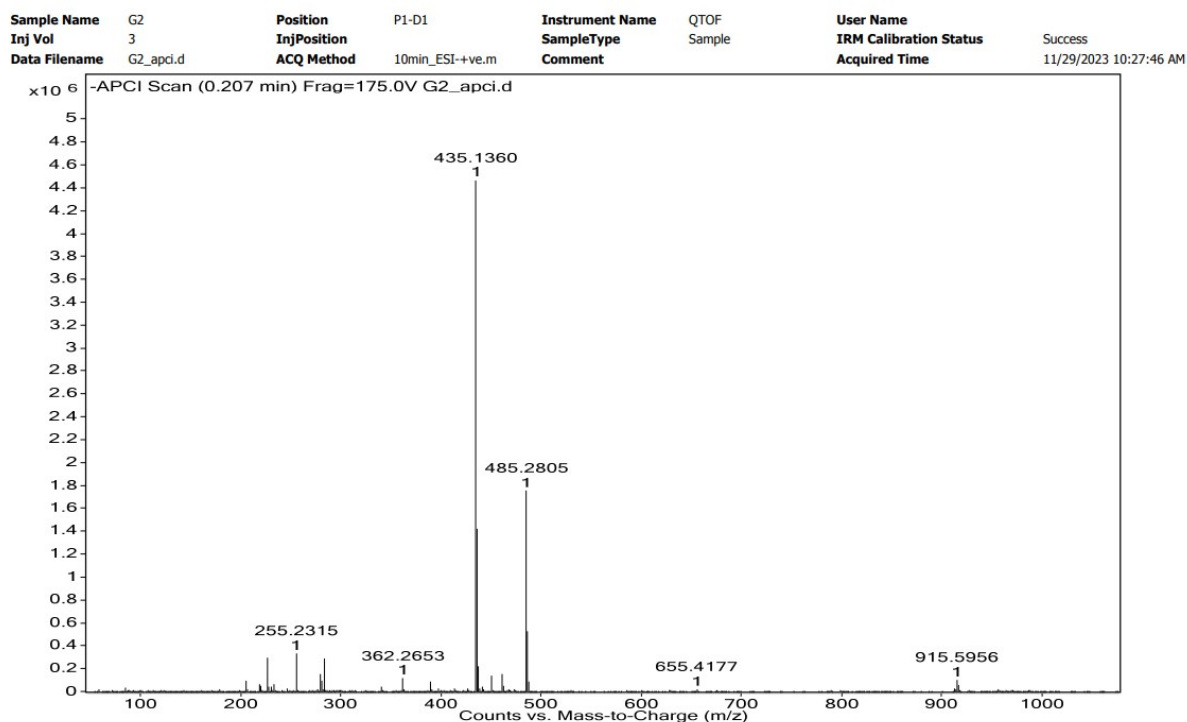


Figure S32. HR-LC-MS spectra of GBY-8.

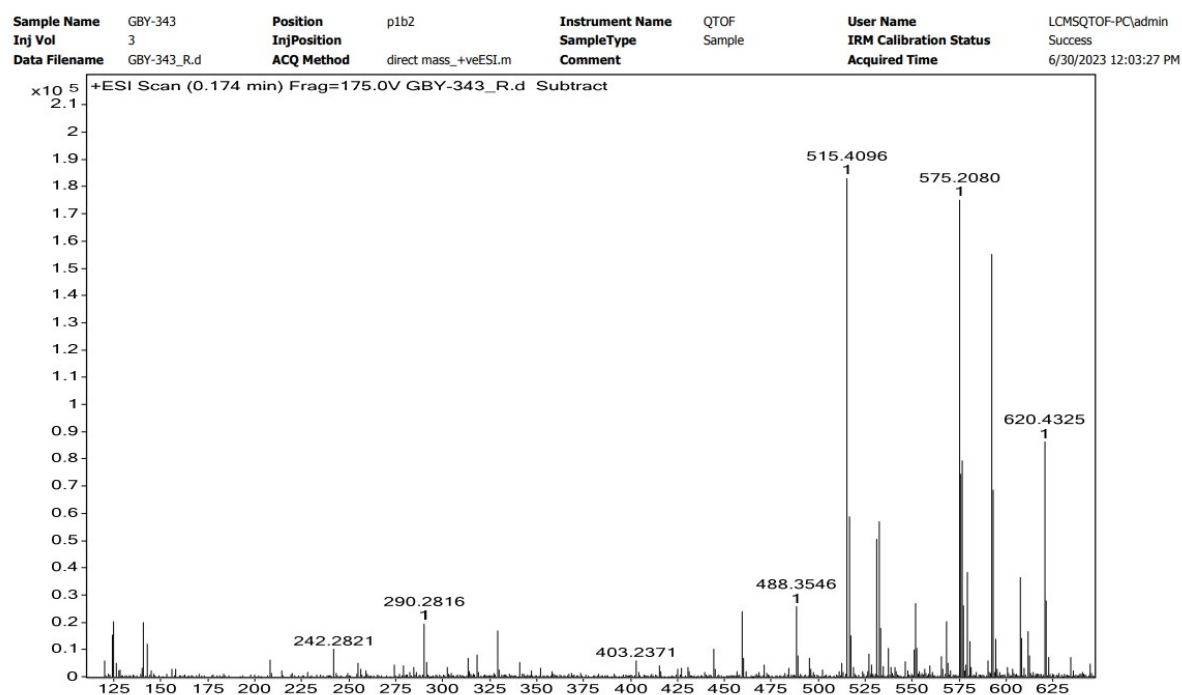


Figure S33. HR-LC-MS spectra of GBY-9.

Single Crystal XRD Analysis of GBY-7 and GBY-9

The Single crystal XRD data has been collected on single crystal X-ray diffractometer of Bruker Smart Apex Duo diffractometer at 100 K using Mo K α radiation ($\lambda = 0.71073 \text{ \AA}$). The frames were integrated with the Bruker SAINT Software package using a narrow-frame

algorithm. Data were corrected for absorption effects using the Multi-Scan method (SADABS). The structure was solved and refined using the Bruker SHELXTL Software Package. The structure figure was generated with ORTEP.

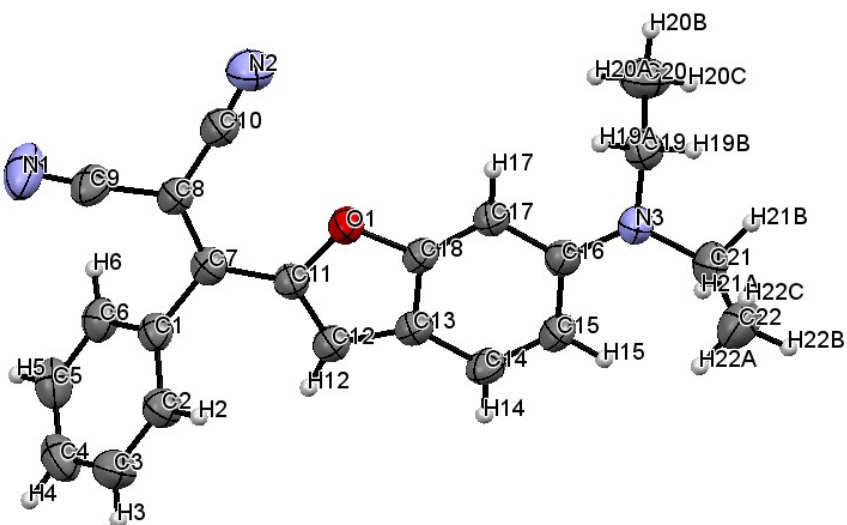


Figure S34. X-Ray crystal structure of **GBY-7** (Ellipsoids with 50% probability).

Table S9. Single crystal data and structure refinement for **GBY-7**.

Identification code	2348042
Empirical formula	C ₂₂ H ₁₉ N ₃ O
Formula weight	341.40
Temperature	296K
Wavelength	0.7107
Crystal system	triclinic
Space group	P-1
Unit cell dimensions	
a(Å)	9.670(4)
b(Å)	9.892(4)
c(Å)	9.990(4)
α(Å)	70.707 (11)
β(Å)	81.349(12)

$\gamma(\text{\AA})$	82.089 (12)
Volume	887.705
Z	2
Density (calculated)	1.277
Absorption coefficient	0.080
F (000)	360
Refinement method	'SHELXL 2019/3 (Sheldrick, 2015)
Data / restraints / parameters	4589/0/237
Goodness-of-fit on F2	0.955
Final R indices [I>2sigma(I)]	R1 = 0.0607, wR2 = 0.1863
R indices (all data)	0.1669

$$R_1 = \frac{\sum \| |F_0| - |F_c| \|}{\sum |F_0|}$$

$$R_w = \sqrt{\frac{[\sum \{w(F_0^2 - F_c^2)^2\}]}{[\sum \{w(F_0^2)^2\}]}}$$

Table S10. List Torsion angles [°] for luminogen GBY-7

Number	Atom1	Atom2	Atom3	Atom4	Torsion
1	C11	O1	C18	C13	0.4(2)
2	C11	O1	C18	C17	179.8(2)
3	C18	O1	C11	C12	-0.6(2)
4	C18	O1	C11	C7	-178.2(2)
5	C21	N3	C16	C17	-179.0(2)
6	C21	N3	C16	C15	1.2(3)
7	C19	N3	C16	C17	0.6(3)

8	C19	N3	C16	C15	-179.2(2)
9	C16	N3	C21	H21A	34.9
10	C16	N3	C21	H21B	152.3
11	C16	N3	C21	C22	-86.4(3)
12	C19	N3	C21	H21A	-144.7
13	C19	N3	C21	H21B	-27.3
14	C19	N3	C21	C22	93.9(3)
15	C16	N3	C19	H19A	32.2
16	C16	N3	C19	H19B	149.8
17	C16	N3	C19	C20	-89.0(3)
18	C21	N3	C19	H19A	-148.2
19	C21	N3	C19	H19B	-30.6
20	C21	N3	C19	C20	90.6(3)
21	O1	C18	C13	C12	-0.1(2)
22	O1	C18	C13	C14	179.3(2)
23	C17	C18	C13	C12	-179.5(2)
24	C17	C18	C13	C14	-0.1(3)
25	O1	C18	C17	H17	0.2
26	O1	C18	C17	C16	-179.7(2)
27	C13	C18	C17	H17	179.5
28	C13	C18	C17	C16	-0.4(4)
29	O1	C11	C12	C13	0.6(2)
30	O1	C11	C12	H12	-179.5
31	C7	C11	C12	C13	177.8(2)
32	C7	C11	C12	H12	-2.2
33	O1	C11	C7	C1	-174.9(2)

34	O1	C11	C7	C8	5.8(3)
35	C12	C11	C7	C1	8.1(3)
36	C12	C11	C7	C8	-171.2(2)
37	C18	C13	C12	C11	-0.3(2)
38	C18	C13	C12	H12	179.7
39	C14	C13	C12	C11	-179.5(2)
40	C14	C13	C12	H12	0.5
41	C18	C13	C14	H14	-179
42	C18	C13	C14	C15	1.1(3)
43	C12	C13	C14	H14	0.1
44	C12	C13	C14	C15	-179.8(2)
45	C2	C1	C7	C11	56.9(3)
46	C2	C1	C7	C8	-123.8(3)
47	C6	C1	C7	C11	-121.7(2)
48	C6	C1	C7	C8	57.6(3)
49	C7	C1	C2	H2	1.7
50	C7	C1	C2	C3	-178.3(2)
51	C6	C1	C2	H2	-179.7
52	C6	C1	C2	C3	0.4(4)
53	C7	C1	C6	H6	-2.8
54	C7	C1	C6	C5	177.1(2)
55	C2	C1	C6	H6	178.6
56	C2	C1	C6	C5	-1.5(4)
57	C18	C17	C16	N3	-179.8(2)
58	C18	C17	C16	C15	-0.0(3)
59	H17	C17	C16	N3	0.3

60	H17	C17	C16	C15	-180
61	N3	C16	C15	C14	-179.2(2)
62	N3	C16	C15	H15	0.7
63	C17	C16	C15	C14	1.0(3)
64	C17	C16	C15	H15	-179
65	C10	C8	C7	C11	1.1(4)
66	C10	C8	C7	C1	-178.1(2)
67	C9	C8	C7	C11	-178.4(2)
68	C9	C8	C7	C1	2.4(4)
69	C7	C8	C10	N2	-174(4)
70	C9	C8	C10	N2	6(4)
71	C7	C8	C9	N1	-159(4)
72	C10	C8	C9	N1	21(4)
73	C13	C14	C15	C16	-1.6(3)
74	C13	C14	C15	H15	178.5
75	H14	C14	C15	C16	178.5
76	H14	C14	C15	H15	-1.4
77	C1	C2	C3	H3	-178.8
78	C1	C2	C3	C4	1.1(4)
79	H2	C2	C3	H3	1.3
80	H2	C2	C3	C4	-178.8
81	C1	C6	C5	H5	-178.9
82	C1	C6	C5	C4	1.1(4)
83	H6	C6	C5	H5	1
84	H6	C6	C5	C4	-178.9
85	N3	C21	C22	H22A	61.3

86	N3	C21	C22	H22B	-178.7
87	N3	C21	C22	H22C	-58.7
88	H21A	C21	C22	H22A	-60
89	H21A	C21	C22	H22B	60
90	H21A	C21	C22	H22C	-180
91	H21B	C21	C22	H22A	-177.5
92	H21B	C21	C22	H22B	-57.5
93	H21B	C21	C22	H22C	62.5
94	N3	C19	C20	H20A	60.5
95	N3	C19	C20	H20B	-179.5
96	N3	C19	C20	H20C	-59.5
97	H19A	C19	C20	H20A	-60.8
98	H19A	C19	C20	H20B	59.3
99	H19A	C19	C20	H20C	179.2
100	H19B	C19	C20	H20A	-178.4
101	H19B	C19	C20	H20B	-58.3
102	H19B	C19	C20	H20C	61.6
103	C6	C5	C4	C3	0.4(4)
104	C6	C5	C4	H4	-179.6
105	H5	C5	C4	C3	-179.6
106	H5	C5	C4	H4	0.5
107	C2	C3	C4	C5	-1.5(5)
108	C2	C3	C4	H4	178.4
109	H3	C3	C4	C5	178.4
110	H3	C3	C4	H4	-1.7

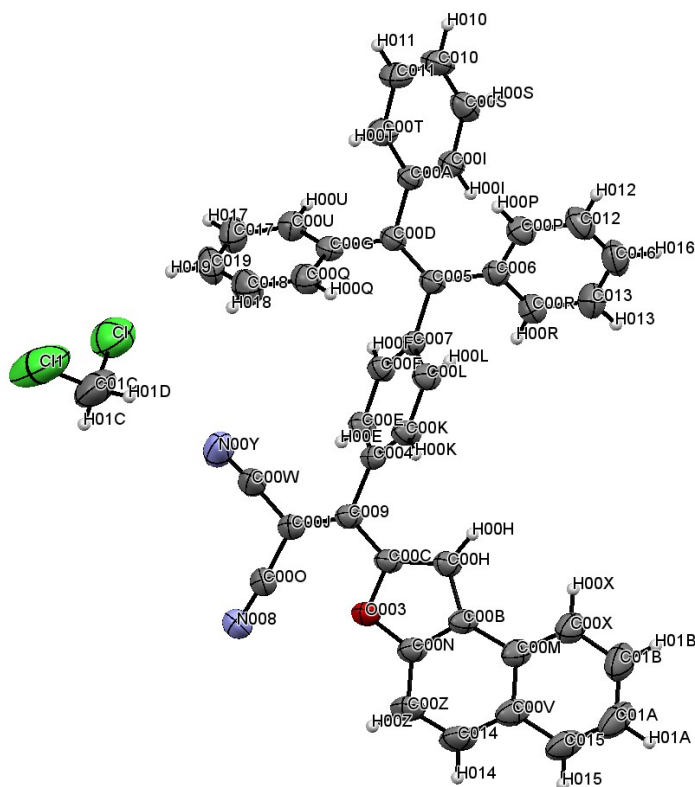


Figure S35. X-Ray crystal structure of **GBY-9** (Ellipsoids with 50% probability).

Table S11. Single crystal data and structure refinement for **GBY-9**.

Identification code	2348040
Empirical formula	$C_{42}H_{26}N_2O \cdot CH_2Cl_2$
Formula weight	$574.68 + 84.93 = 659.60$
Temperature	296K
Wavelength	0.7107
Crystal system	monoclinic
Space group	P 1 21/n 1
Unit cell dimensions	
a(Å)	9.232(2)
b(Å)	23.274 (5)
c(Å)	15.821 (4)

α (Å)	90
β (Å)	91.951 (7)
γ (Å)	90
Volume	3397.4
Z	4
Density (calculated)	1.289
Absorption coefficient	0.228
F(000)	1368
Refinement method	'SHELXL 2019/3 (Sheldrick, 2015)
Data / restraints / parameters	8601/0/433
Goodness-of-fit on F2	1.012
Final R indices [I>2sigma(I)]	R1 = 0.0679, wR2 = 0.1984
R indices (all data)	0.1549

Table S12. List Torsion angles [°] for luminogen GBY-9

Number	Atom1	Atom2	Atom3	Atom4	Torsion
1	C00N	O003	C00C	C009	172.8(2)
2	C00N	O003	C00C	C00H	-0.7(3)
3	C00C	O003	C00N	C00B	0.8(3)
4	C00C	O003	C00N	C00Z	-177.8(3)
5	C00E	C004	C009	C00C	130.2(3)
6	C00E	C004	C009	C00J	-48.8(4)
7	C00K	C004	C009	C00C	-51.2(4)
8	C00K	C004	C009	C00J	129.8(3)
9	C009	C004	C00E	H00E	-4.3
10	C009	C004	C00E	C00F	175.7(2)

11	C00K	C004	C00E	H00E	177.1
12	C00K	C004	C00E	C00F	-2.9(4)
13	C009	C004	C00K	H00K	3
14	C009	C004	C00K	C00L	-177.0(3)
15	C00E	C004	C00K	H00K	-178.3
16	C00E	C004	C00K	C00L	1.7(4)
17	C007	C005	C006	C00P	-134.4(3)
18	C007	C005	C006	C00R	44.9(3)
19	C00D	C005	C006	C00P	46.7(4)
20	C00D	C005	C006	C00R	-133.9(3)
21	C006	C005	C007	C00F	-120.5(3)
22	C006	C005	C007	C00L	59.0(3)
23	C00D	C005	C007	C00F	58.4(4)
24	C00D	C005	C007	C00L	-122.1(3)
25	C006	C005	C00D	C00A	7.2(4)
26	C006	C005	C00D	C00G	-172.3(2)
27	C007	C005	C00D	C00A	-171.6(2)
28	C007	C005	C00D	C00G	8.9(4)
29	C005	C006	C00P	H00P	0.8
30	C005	C006	C00P	C012	-179.3(3)
31	C00R	C006	C00P	H00P	-178.6
32	C00R	C006	C00P	C012	1.3(4)
33	C005	C006	C00R	H00R	-1.5
34	C005	C006	C00R	C013	178.6(3)
35	C00P	C006	C00R	H00R	177.9
36	C00P	C006	C00R	C013	-2.1(4)

37	C005	C007	C00F	C00E	-178.0(2)
38	C005	C007	C00F	H00F	2
39	C00L	C007	C00F	C00E	2.5(4)
40	C00L	C007	C00F	H00F	-177.5
41	C005	C007	C00L	C00K	176.7(3)
42	C005	C007	C00L	H00L	-3.2
43	C00F	C007	C00L	C00K	-3.8(4)
44	C00F	C007	C00L	H00L	176.3
45	C004	C009	C00C	O003	169.2(2)
46	C004	C009	C00C	C00H	-18.9(4)
47	C00J	C009	C00C	O003	-11.8(4)
48	C00J	C009	C00C	C00H	160.1(3)
49	C004	C009	C00J	C00O	-180.0(3)
50	C004	C009	C00J	C00W	0.6(4)
51	C00C	C009	C00J	C00O	1.1(4)
52	C00C	C009	C00J	C00W	-178.4(3)
53	C00I	C00A	C00D	C005	45.6(4)
54	C00I	C00A	C00D	C00G	-134.9(3)
55	C00T	C00A	C00D	C005	-136.8(3)
56	C00T	C00A	C00D	C00G	42.7(4)
57	C00D	C00A	C00I	H00I	-2.6
58	C00D	C00A	C00I	C00S	177.4(3)
59	C00T	C00A	C00I	H00I	179.7
60	C00T	C00A	C00I	C00S	-0.3(4)
61	C00D	C00A	C00T	H00T	2.2
62	C00D	C00A	C00T	C011	-177.7(3)

63	C00I	C00A	C00T	H00T	179.9
64	C00I	C00A	C00T	C011	-0.0(4)
65	C00M	C00B	C00H	C00C	176.1(3)
66	C00M	C00B	C00H	H00H	-3.9
67	C00N	C00B	C00H	C00C	0.1(3)
68	C00N	C00B	C00H	H00H	-179.9
69	C00H	C00B	C00M	C00V	-175.7(3)
70	C00H	C00B	C00M	C00X	2.2(5)
71	C00N	C00B	C00M	C00V	-0.1(4)
72	C00N	C00B	C00M	C00X	177.8(3)
73	C00H	C00B	C00N	O003	-0.6(3)
74	C00H	C00B	C00N	C00Z	178.0(3)
75	C00M	C00B	C00N	O003	-177.3(2)
76	C00M	C00B	C00N	C00Z	1.2(4)
77	O003	C00C	C00H	C00B	0.4(3)
78	O003	C00C	C00H	H00H	-179.6
79	C009	C00C	C00H	C00B	-172.0(3)
80	C009	C00C	C00H	H00H	8
81	C005	C00D	C00G	C00Q	48.6(4)
82	C005	C00D	C00G	C00U	-133.7(3)
83	C00A	C00D	C00G	C00Q	-130.9(3)
84	C00A	C00D	C00G	C00U	46.8(4)
85	C004	C00E	C00F	C007	0.9(4)
86	C004	C00E	C00F	H00F	-179.1
87	H00E	C00E	C00F	C007	-179.2
88	H00E	C00E	C00F	H00F	0.9

89	C00D	C00G	C00Q	H00Q	-0.9
90	C00D	C00G	C00Q	C018	179.0(3)
91	C00U	C00G	C00Q	H00Q	-178.7
92	C00U	C00G	C00Q	C018	1.2(4)
93	C00D	C00G	C00U	H00U	0
94	C00D	C00G	C00U	C017	-179.9(3)
95	C00Q	C00G	C00U	H00U	177.8
96	C00Q	C00G	C00U	C017	-2.1(5)
97	C00A	C00I	C00S	H00S	-179
98	C00A	C00I	C00S	C010	1.0(5)
99	H00I	C00I	C00S	H00S	1
100	H00I	C00I	C00S	C010	-179
101	C009	C00J	C00O	N008	173(4)
102	C00W	C00J	C00O	N008	-8(4)
103	C009	C00J	C00W	N00Y	168(5)
104	C00O	C00J	C00W	N00Y	-12(6)
105	C004	C00K	C00L	C007	1.7(4)
106	C004	C00K	C00L	H00L	-178.3
107	H00K	C00K	C00L	C007	-178.3
108	H00K	C00K	C00L	H00L	1.6
109	C00B	C00M	C00V	C014	-0.7(4)
110	C00B	C00M	C00V	C015	178.4(3)
111	C00X	C00M	C00V	C014	-178.7(3)
112	C00X	C00M	C00V	C015	0.4(4)
113	C00B	C00M	C00X	H00X	2.3
114	C00B	C00M	C00X	C01B	-177.6(3)

115	C00V	C00M	C00X	H00X	-179.8
116	C00V	C00M	C00X	C01B	0.2(5)
117	O003	C00N	C00Z	H00Z	-3.1
118	O003	C00N	C00Z	C014	176.9(3)
119	C00B	C00N	C00Z	H00Z	178.5
120	C00B	C00N	C00Z	C014	-1.5(5)
121	C006	C00P	C012	H012	-179.9
122	C006	C00P	C012	C016	0.2(5)
123	H00P	C00P	C012	H012	0
124	H00P	C00P	C012	C016	-179.9
125	C00G	C00Q	C018	H018	-179.6
126	C00G	C00Q	C018	C019	0.3(5)
127	H00Q	C00Q	C018	H018	0.3
128	H00Q	C00Q	C018	C019	-179.7
129	C006	C00R	C013	H013	-178.5
130	C006	C00R	C013	C016	1.3(5)
131	H00R	C00R	C013	H013	1.5
132	H00R	C00R	C013	C016	-178.6
133	C00I	C00S	C010	H010	178.6
134	C00I	C00S	C010	C011	-1.4(5)
135	H00S	C00S	C010	H010	-1.5
136	H00S	C00S	C010	C011	178.6
137	C00A	C00T	C011	C010	-0.4(5)
138	C00A	C00T	C011	H011	179.6
139	H00T	C00T	C011	C010	179.6
140	H00T	C00T	C011	H011	-0.4

141	C00G	C00U	C017	H017	-178.5
142	C00G	C00U	C017	C019	1.4(5)
143	H00U	C00U	C017	H017	1.6
144	H00U	C00U	C017	C019	-178.5
145	C00M	C00V	C014	C00Z	0.5(5)
146	C00M	C00V	C014	H014	-179.6
147	C015	C00V	C014	C00Z	-178.6(3)
148	C015	C00V	C014	H014	1.3
149	C00M	C00V	C015	H015	179.7
150	C00M	C00V	C015	C01A	-0.4(5)
151	C014	C00V	C015	H015	-1.1
152	C014	C00V	C015	C01A	178.7(3)
153	C00M	C00X	C01B	C01A	-0.9(5)
154	C00M	C00X	C01B	H01B	179.2
155	H00X	C00X	C01B	C01A	179.1
156	H00X	C00X	C01B	H01B	-0.8
157	C00N	C00Z	C014	C00V	0.6(5)
158	C00N	C00Z	C014	H014	-179.4
159	H00Z	C00Z	C014	C00V	-179.4
160	H00Z	C00Z	C014	H014	0.7
161	C00S	C010	C011	C00T	1.1(5)
162	C00S	C010	C011	H011	-178.9
163	H010	C010	C011	C00T	-178.9
164	H010	C010	C011	H011	1.2
165	C00P	C012	C016	C013	-1.0(5)
166	C00P	C012	C016	H016	179.1

167	H012	C012	C016	C013	179.1
168	H012	C012	C016	H016	-0.8
169	C00R	C013	C016	C012	0.3(5)
170	C00R	C013	C016	H016	-179.9
171	H013	C013	C016	C012	-179.9
172	H013	C013	C016	H016	0
173	C00V	C015	C01A	H01A	179.7
174	C00V	C015	C01A	C01B	-0.3(6)
175	H015	C015	C01A	H01A	-0.4
176	H015	C015	C01A	C01B	179.6
177	C00U	C017	C019	C018	0.2(6)
178	C00U	C017	C019	H019	-179.7
179	H017	C017	C019	C018	-179.8
180	H017	C017	C019	H019	0.2
181	C00Q	C018	C019	C017	-1.1(6)
182	C00Q	C018	C019	H019	178.9
183	H018	C018	C019	C017	178.9
184	H018	C018	C019	H019	-1.1
185	C015	C01A	C01B	C00X	0.9(6)
186	C015	C01A	C01B	H01B	-179.2
187	H01A	C01A	C01B	C00X	-179.1
188	H01A	C01A	C01B	H01B	0.8